Green Chemistry

ROYAL SOCIETY OF CHEMISTRY

CRITICAL REVIEW

View Article Online
View Journal | View Issue

Cite this: *Green Chem.*, 2024, **26**, 10661

Rhenium-based catalysts for biomass conversion

Julian Skagfjörd Reinhold,[a,b] Jifeng Pang,*[a] Bo Zhang,*[a] Fritz E. Kühn*[b] and Tao Zhang[a]

Received 17th June 2024,
Accepted 13th September 2024

DOI: 10.1039/d4gc02925a

rsc.li/greenchem

Biomass is the most abundant and renewable resource in the pursuit of bio-value added chemicals. Platinum-group metals and typical nonprecious transition metals are considered as the active metals for catalytic conversion of biomass into value added chemicals and fuels. Rhenium (Re) in particular is a versatile, oxophilic element with a broad variety of easily accessible oxidation states ideally suited for catalytic applications. Taking advantage of Re's unique properties and the green concept of biomass, the catalytic transformation of lignocellulose with Re-based catalysts has gained considerable attention, leading to the preparation of value-added chemicals including olefins through deoxydehydration from the conversion of polyols, aromatics through depolymerization of lignin, and alkane fuels through a hydrodeoxygenation reaction. This review focuses on the catalytic conversion of lignocellulosic main components (cellulose, hemicellulose, and lignin) and their derived platform chemicals into value-added chemicals and fuels over homogeneous and heterogeneous Re-based catalysts. The reaction pathways for biomass conversion over Re-based catalysts are introduced based on different feedstocks or chemical bonds. The unique role of Re species in tailoring the active sites of catalysts for these reactions is summarized and possible reaction mechanisms are discussed. Finally, an outlook is provided to underscore both the challenges and opportunities associated with this interesting and important field, offering a comprehensive overview on the current state of Re catalysis with a low carbon footprint.

1. Introduction

The excessive consumption of fossil resources increases CO_2 emissions, inducing global climate change and several other serious environmental issues. Since the Paris Agreement was signed in 2015, an increasing number of countries have pledged to limit CO_2 emissions and now regard carbon neutrality as a national strategy.[1] To achieve this ambitious goal, renewable energy resources such as solar, wind, hydro, biomass, tidal, geothermal, and ocean thermal, are gradually incorporated into energy systems to approach a future without further consumption of fossil feedstock.[2,3] As the only carbon-containing renewable energy resource, biomass is an ideal resource for upgrading into a variety of valuable chemicals, fuels and materials, gradually replacing the current fossil sources also as a basis for the chemical industry.[4–7]

Biomass, mainly lignocellulosic biomass, is composed of cellulose (30–50%), hemicellulose (20–40%), and lignin (10–30%).[8,9] Cellulose and hemicellulose are polysaccharides with basic units of pentose and hexose, respectively, linked by glycosidic bonds.[9] Lignin is a polymer of aromatic alcohols that is branched and has different C–O and C–C bond combinations.[10] In plant cells, these three components interact strongly to form a rigid structure *via* hydrogen and covalent bonds and are hard to degrade under chemical and biological conditions. In recent decades, significant progress has been made in the development of novel catalysts and the study of reaction mechanisms, aimed at efficiently and selectively converting biomass into value-added products.[5,9,11,12] Considering the different structures of (hemi)cellulose and lignin, most works first separate these components from lignocellulosic biomass and afterwards transform them into platform chemicals *via* chemical or biological methods, followed by further upgrading into key chemicals and fuels. Specifically, the oxygen-containing functional groups in biomass or platform chemicals are treated with metal and/or oxide catalysts *via* hydrodeoxygenation, hydrogenolysis, decarbonylation, decarboxylation, oxidation, esterification, isomerization, dehydration and hydrolysis reactions to meet the current requirements for achieving industrially useful chemical compounds.[13] For instance, (hemi)cellulose or lignin is catalytically converted into glycols, furfural, 5-hydroxymethylfurfural or aromatics, and then upgraded into fine chemicals and advanced fuels, or the carbohydrates in biomass are fermented into alcohols and carboxylic acids for further catalytic conversions.[14–16]

[a]*CAS Key Laboratory of Science and Technology on Applied Catalysis, Dalian Institute of Chemical Physics, Chinese Academy of Sciences, Dalian 116023, China. E-mail: jfpang@dicp.ac.cn, bo.zhang@dicp.ac.cn*
[b]*Molecular Catalysis, Department of Chemistry and Catalysis Research Center, TUM School of Natural Sciences, Technical University of Munich, Lichtenbergstr. 4, D-85748 Garching bei München, Bavaria, Germany. E-mail: fritz.kuehn@ch.tum.de*

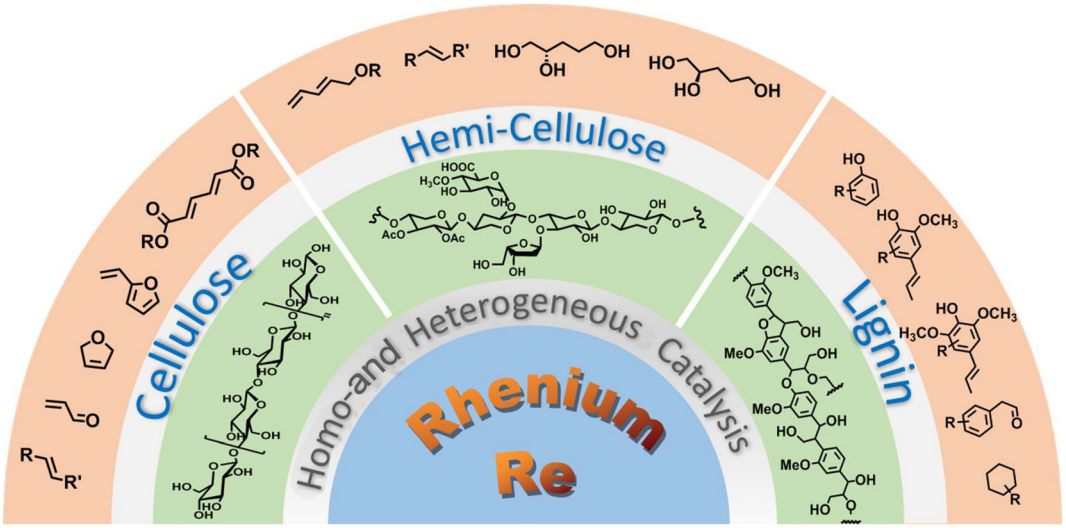

Fig. 1 Overview of biomass conversion over homogeneous and heterogeneous Re-based catalysts.

During these catalytic processes, transition metal catalysts have gained great attention due to their specific electronic structure and ability to easily give or take electrons from other molecules. Among them, rhenium (Re) is a versatile element and has widely been applied in catalyzing oxygen-containing functional groups in biomass conversions.[17,18] Because Re has a variety of easily accessible oxidation states, it provides a number of possibilities to adjust the interaction between catalysts and biomass-derived substrates.[19] Typically, organometallic Re species like organo(trioxo-Re) complexes demonstrate soft "enzyme-like" structures for deoxydehydration reactions.[20–25] Furthermore, ReO_x have acidic, oxophilic and metallic properties and demonstrate great potential in dissociating H_2 molecules or suitable interactions for –OH containing compounds' conversion. Thus, Re species are used directly as a notable promoter to modify the coordination environment, electronic structure and acid–base properties of other metal catalysts in typical redox reactions, including dehydration,[26] hydrogenation,[27–29] hydrogenolysis,[30,31] hydrodeoxygenation[32,33] and deoxydehydration reactions.[24,29,34]

Because of the versatile application of Re-based catalysts, several reviews have been dedicated to this topic. For instance, Dilworth provided a detailed review of recent developments in Re chemistry from 2015 to 2020 concerning properties and applications.[19] Raju *et al.* reviewed recent progress in dehydration and deoxydehydration reactions of biomass-derived alcohols and polyols into olefins over Re-based catalysts.[26] DeNike and Kilyanek surveyed the mechanism of the deoxydehydration reaction over homogeneous early metal-oxo catalysts.[35] Recently, the achievements in the deoxydehydration reaction were revisited over transition metal-based catalysts for upgrading bio-based polyols into value-added chemicals and fuels.[22,36,37] However, most of the reviews focus on some specific reactions. Highlighting the achievements in the catalytic conversion of biomass over both homogeneous and heterogeneous Re-based catalysts has not yet been covered, especially with the newly emerging lignin depolymerization reactions[38–44] and raw lignocellulosic biomass upgrading.[45]

In this review, the application of Re-based catalysts for biomass conversion including cellulosic biomass, lignin, and platform chemicals catalyzed by homogeneous and heterogeneous Re-based catalysts is comprehensively reviewed and discussed (Fig. 1). In detail, catalytic conversion of sugar derivatives and lignin is first introduced, focusing on homogeneous organic Re complexes and the discussion of mechanistic studies. Then, works on the conversion of hemicellulose, lignin and platform chemicals over heterogeneous Re catalysts are discussed from the viewpoint of the key role of Re species in tailoring different reaction pathways. Moreover, challenges and opportunities for biomass conversions over Re-based catalysts are addressed. This review offers a useful resource to explore alternative Re-based catalysts for biomass conversion in industrial applications and to encourage researchers to develop feasible, sustainable and economical technologies to maximize the chemical, fuel and material production from biomass feedstock.

2. Homogeneous Re-based catalysts for biomass conversion

Subdividing catalysis into homogeneous and heterogeneous reactions is a traditional approach, relating to the thermodynamic phases of catalyst and reactants. The characteristic feature of homogeneous catalysis is the coexistence of the catalyst and reactants in the same phase, which leads to high catalytic efficiency owing to sufficient contact between the active center and reactants and only a small influence of diffusion, as long as enough substrate is available in the proximity of the

catalyst.[46] Additionally, homogeneous catalysis allows for the catalytic selectivity to be rationally tuned by adjusting the ligand associated with the active metal. However, separating homogeneous catalysts from the reaction can be challenging and/or associated with considerable energy consumption, which limits industrial applications. Another issue is that homogeneous catalysis is usually not well compatible for continuous processes.

Notwithstanding these limitations, homogeneous Re-based compounds and their applications have gained quite some interest during recent decades.[19,47–49] In particular, organorhenium oxides are in rapid progress in both catalysis and materials science,[47,49–52] producing a large number of useful active and selective Re-complex candidates for catalytic reactions. For instance, methyltrioxorhenium(VII) is utilized as an oxidation catalyst with a wide variety of applications, displaying robust activity and product selectivity.[53–55] Building upon this highly promising foundation, there has been a rapid increase in studies focusing on organometallic derivatives and their catalytic reactions. While extensive reviews have covered aspects such as synthesis, structure, spectroscopy, and chemical behavior, recent attention has been directed towards exploring new applications, particularly in the realm of biomass conversion. In this section, particular emphasis is given to biomass conversion catalyzed by homogeneous Re-based catalysts.

2.1 Conversion of (hemi)cellulose

Cellulose is a polymer that is both chemically stable and insoluble in the majority of solvents, since glucose is joined by β-1,4-glycosidic linkages to form a strong crystal structure with a network of intra- and intermolecular H-bonds.[56,57] Thus, it is still a challenge to degrade cellulose into target products with high efficiency.[58] In contrast, monosaccharides derived from carbohydrates are preferably selected as model substrates for catalytic conversions because of their good solubility and enhanced reactivity. In addition, previous works show that homogeneous organometallic Re compounds have outstanding performance in removing hydroxy groups, especially in the deoxydehydration reaction, which allows the removal of two adjacent hydroxy groups from diols, leading to an olefin in the presence of a reducing agent.[17,24] Since deoxydehydration reactions of polyols (<C4) catalyzed by homogeneous Re-based catalysts have already been reviewed,[22,24] the focus of this part is on the summary of deoxydehydration reactions, categorized by sugar, sugar alcohols and sugar acids (>C3) along with the typical ranges of reaction conditions.

2.1.1 Sugars. Glucose is the major cellulose component and widely employed as a substrate for the production of olefins through deoxydehydration reactions. Methyltrioxorhenium catalyzes the conversion of D-glucose with 3-pentanol as the reducing agent, reaching a 25% yield of 2-vinylfuran and furan at a ratio of 1 : 1.8 (Table 1, entry 1).[59] Substituted homogeneous Re-based catalysts also enable deoxydehydration reactions towards olefins. For instance, cyclopentadiene substituted homogeneous Re ($Cp^{tt}ReO_3$) (Cp^{tt} = 1,3-di-*tert*-butylcyclopentadienyl) and $L^4Re(CO)_3$ (L^4 = 2,4-di-*tert*-butyl-6-(tetramethylethane-1,2-diamine)phenol) can be applied for the conversion of D-glucose, yielding 8% and 6% 2-vinylfuran and furan at a ratio of 1.7 : 1 and 1.8 : 1, respectively (Table 1, entry 1).[60,61] The low yield of product using sugar as the feedstock might be attributed to difficulties in coordination of the catalyst and substrate due to the multitude of isomeric states and the thermal instability of substrates.[59] Besides D-glucose, other monosaccharides like D-galactose, D-mannose and D-allose can also be converted to 2-vinylfuran and furan applying these Re-based catalysts. Up to 40% yield of products in the deoxydehydration reaction were achieved (Table 1, entries 2–4).[59,60] In addition, D-xylose and L-arabinose catalyzed by methyltrioxorhenium leads to the ether 2-((octan-3-yloxy)mehtyl)furan as the main product, however in rather low yields (<7%), presumably owing to the reactivity of furfuryl alcohol (Table 1, entries 5 and 6). On the other hand, the deoxydehydration reaction of D-erythrose and D-threose catalyzed by methyltrioxorhenium results in 60% and 47% furan yields, respectively (Table 1, entries 7 and 8). This comparatively high yield is attributed to two reactions occurring within the system, including a deoxydehydration reaction of two carbon, C1 and C2, with hydroxy groups, and the epimerization of the C2 hydroxy group *via* erythrulose.[59] Based on the aforementioned findings, achieving a high yield of olefins from the deoxydehydration reaction of sugars remains a significant challenge. This is primarily attributed to the complex structure of sugars, which leads to an equilibrium between multiple isomeric forms, coupled with their thermal instability under hydrothermal conditions.

2.1.2 Sugar alcohols. Sugar alcohols including glycerol, xylitol, and sorbitol, are promising renewable resources for the production of value-added chemicals. Xylitol and sorbitol can be obtained from the hydrogenation of xylose and glucose or hemicellulose and cellulose, while glycerol is produced as a by-product from biodiesel in considerable amounts. Deoxydehydration of sugar alcohols into the corresponding olefins can therefore be understood as a direct path for utilization of biomass in the chemical industry and as enabling the biorefinery concept. For example, xylitol, D-arabinitol, ribitol, D-sorbitol and D-mannitol can be transformed to the corresponding olefin products with methyltrioxorhenium as the catalyst in the presence of 3-pentanol (Fig. 2).[59] Additionally, cyclopentadiene substituted $Cp^{tt}ReO_3$ (Cp^{tt} = 1,3-di-*tert*-butylcyclopentadienyl) is also active for the transformation of D-mannitol to 1,3,5-hexatriene in 35% yield at 135 °C within 15 h in 3-octanol through a deoxydehydration reaction. Similarly, D-arabinitol can be converted to penta-2,4-dien ether in 48% yield when applying the same conditions.[61]

Both glucose fermentation and pentose decarbonylation produces erythritol alcohol,[62] which is therefore regarded as a platform chemical in a biomass refinery. A variety of C_4 chemicals can be obtained from erythritol, of which the deoxydehydration reaction of erythritol to alkenes has caught rapidly growing attention. Homogeneous Re-based catalysts with a reducing agent, such as methyltrioxorhenium with 3-octanol,

Table 1 Deoxydehydration reactions of various sugars

Entry	Substrate	Catalyst	Product	Yield	Reducing agent	Reaction conditions	Ref.
1	D-Glucose	 (MTO)	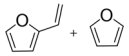	25% (1 : 1.8)	3-Pentanol	155 °C, 3 h, N_2	59
		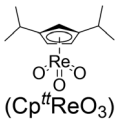 ($Cp^{tt}ReO_3$)		8% (1.7 : 1)	3-Octanol	135 °C, 15 h, N_2	61
		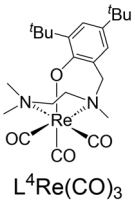 $L^4Re(CO)_3$		6% (1.8 : 1)	3-Pentanol	155 °C, 3 h, air	60
2	D-Galactose	MTO $Cp^{tt}ReO_3$ $L^4Re(CO)_3$	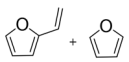	32% (1 : 3.0) 22% (1.2 : 1) 11% (2.0 : 1)	3-Pentanol 3-Octanol 3-Pentanol	155 °C, 3 h, N_2 135 °C,15 h, N_2 155 °C, 3 h, air	59 61 60
3	D-Mannose	MTO $Cp^{tt}ReO_3$ $L^4Re(CO)_3$	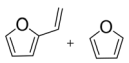	30% (1 : 2.3) 39% (2.3 : 1) 32% (1.5 : 1)	3-Pentanol 3-Pentanol 3-Pentanol	155 °C, 3 h, N_2 155 °C, 12 h, N_2 155 °C, 3 h, air	59 61 60
4	D-Allose	MTO	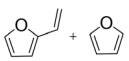	40% (1 : 2.1)	3-Pentanol	155 °C, 3 h, N_2	59
5	D-Xylose	MTO	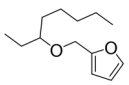	Trace	3-Octanol	155 °C, 2 h, N_2	59
6	L-Arabinose	MTO	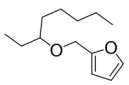	7%	3-Octanol	155 °C, 2 h, N_2	59
7	D-Erythrose	MTO		60%	3-Octanol	155 °C, 1.25 h, N_2	59
8	L-Threose	MTO		47%	3-Octanol	155 °C, 1.25 h, N_2	59

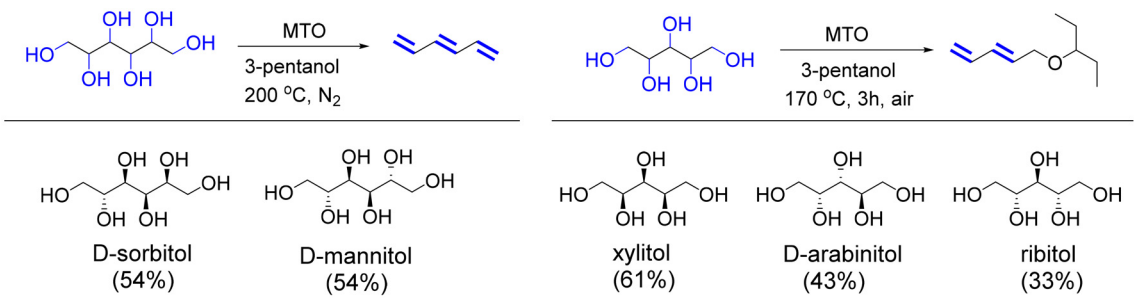

Fig. 2 Deoxydehydration reactions of typical C6 and C5 sugar alcohols[59] (MTO: methyltrioxorhenium).

1-heptanol or indoline, $(NBu_4)ReO_4$ with Na_2SO_3, or $L^4Re(CO)_3$ with 3-octanol can be employed for the deoxydehydration reaction of erythritol. Typical product distributions and reaction conditions are summarized in Fig. 3. With Re-based catalysts, many olefinic products can be obtained in good yields. In detail, methyltrioxorhenium enables the double deoxydehydration of erythritol to 1,3-butadiene in 89% yield within 1.5 h at 167 °C. The reaction, maintained by the reducing agent 3-octanol, also yields 11% 2,5-dihydrofuran as the deoxydehydration coupled dehydration (DH) product.[59] Additionally, reducing agents also greatly affect the deoxydehydration reaction of polyols when utilizing the same Re catalysts. For instance, $(NBu_4)ReO_4$ catalyzes the transformation of tetrol erythritol to olefins with Na_2SO_3 as a reductant at 150 °C within

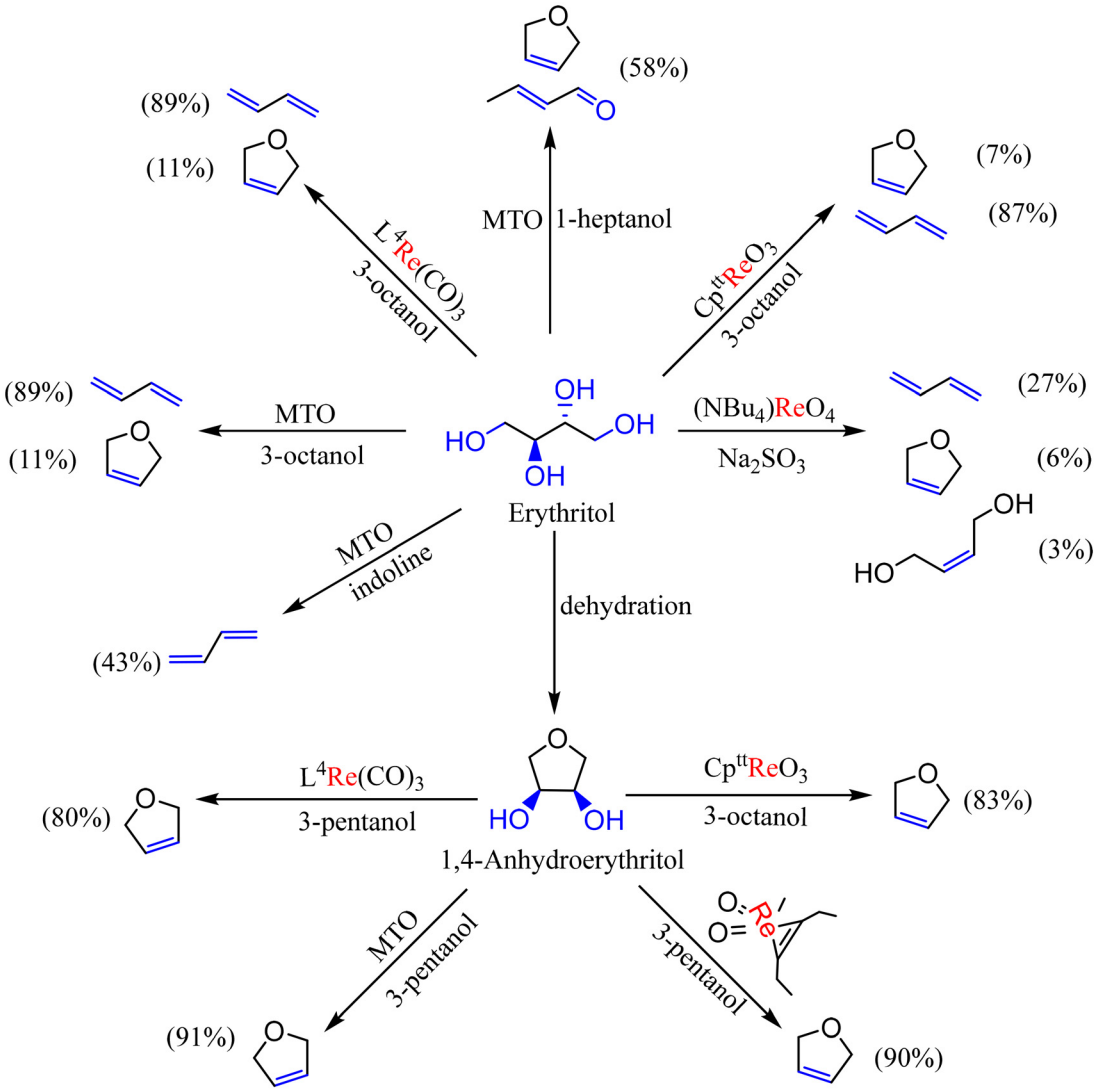

Fig. 3 Erythritol conversion catalyzed by homogeneous Re compounds (MTO: methyltrioxorhenium).

100 h. This process leads to a liquid biphasic mixture, ultimately resulting in a 27% yield of 1,3-butadiene.[63] Utilizing 3-octanol as the reductant, Li *et al.* also have been able to show that $L^4Re(CO)_3$ is efficient in converting erythritol to butadiene with a yield up to 78% at 180 °C within 3 h under air.[60] Similarly, with 1-heptanol as the reductant, *meso*-erythritol can be converted into 2,5-dihydrofuran and allyl alcohol at a total yield of 58% in a 1 : 0.28 ratio using methyltrioxorhenium as the catalyst. However, keeping the reaction for 1 h at 165 °C does not lead to higher product yields.[18] When indoline is used as the reducing agent, erythritol is also converted into 1,3-butadiene in 43% yield with methyltrioxorhenium as the catalyst. After 4 h of reaction at 170 °C, 61% of the oxidized indole compounds are obtained, when using 1-butanol as the solvent.[64] 1,4-Anhydroerythritol, obtained through the dehydration of erythritol, is efficiently converted to 2,5-dihydrofuran in more than 80% yield with catalytic amounts of organorhenium compounds including methyltrioxorhenium, $Cp^{tt}ReO_3$ and $L^4Re(CO)_3$.

When vegetable oils are transesterified to produce biodiesel fuel on a big scale, the primary waste is glycerol. Because of its distinct structural characteristics, chemoselective transformation will produce a variety of platform molecules, including acrolein,[65] hydroxyacetone,[66] propanediols,[67] propene,[68] and propane.[69] Besides these products, allyl alcohol, obtained through the deoxydehydration reaction of glycerol has emerged as a sustainable and economically viable alternative. Most works focus on Re-based catalysts including NH_4ReO_4, $HReO_3$, methyltrioxorhenium and $L^4Re(CO)_3$ for the deoxydehydration reaction of glycerol. The experimental data and reaction conditions are summarized in Table 2. In detail, methyltrioxorhenium is able to catalytically transform glycerol into the corresponding allyl alcohol in yields ranging from 66% to 90% in the presence of a reducing agent (Table 2, entries 1–5). The N,N,O coordinated Re complex (Table 2, entry 6) shows outstanding performance for

Table 2 Deoxydehydration reaction of glycerol to allyl alcohol over Re-based catalysts

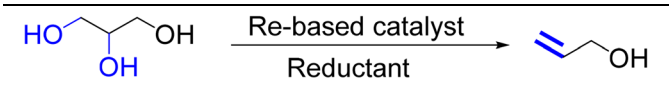

Entry	Catalyst	Reductant	Yield	Condition	Ref.
1	MTO	Glycerol	54%	165 °C, 1 h air	18
2	MTO	3-Octanol	90%	170 °C, 2.5 h air	59
3	MTO	3-Octanol	70%	170 °C, 2.5 h air	71
4	MTO	DMP	87%	140 °C, 16.5 h, H_2	70
5	MTO	Indoline	66%	150 °C, 24 h, N_2	64
6	$L^4Re(CO)_3$	3-Octanol	97%	180 °C, 3 h, air	60
7	$KReO_4$	Glycerol	17%	165 °C, 10 h air	18
8[a]	$NaReO_4$	Glycerol	76%	165 °C, 1 h air	18
9[b]	NH_4ReO_4	Glycerol	75%	165 °C, 1.5 h air	18
10	NH_4ReO_4	3-Octanol	59%	170 °C, 2.5 h air	71
11	NH_4ReO_4	Indoline	80%	150 °C, 24 h, N_2	64
12	ReO_3	DMP	91%	140 °C, 11.5 h, H_2	70
13	ReO_3	DMP	91%	140 °C, 13.5 h, H_2	72

[a] NH_4Cl as additive. [b] KCl as additive; L^4 = 2,4-di-*tert*-butyl-6-(tetramethylethane-1,2-diamine)phenol; DMP = 2,4-dimethyl-3-pentanol. MTO = methyltrioxorhenium.

the deoxydehydration reaction, leading to 97% yield of allyl alcohol at 180 °C within 3 h.[60] Likewise, inorganic salts including $KReO_4$, $NaReO_4$, and NH_4ReO_4 and ReO_3 also enable the catalytic transformation of glycerol into allyl alcohol in acceptable yields (Table 2, entries 7–13).[18,64,70–72]

2.1.3 Sugar acids. Sugar acids are monosaccharides characterized by the presence of a carboxyl group at the end of their chain. As shown in Fig. 4, sugar acids are mainly aldonic acids, ulosonic acids, uronic acids and aldaric acids, which are regarded as sugar-derived building blocks. Considering that sugar acids contain multiple –OH groups, removing two adjacent –OH groups to produce olefins through a deoxydehydration reaction, and then hydrogenation of the C=C bond to obtain the aliphatic diacid is very attractive owing to the wide application of aliphatic diacids in biodegradable polymer sectors. Coupling these cascade steps provides a sustainable and promising strategy for the production of bio-acids.

Glucaric and mucic acids are C_6 sugar acids or aldaric acids, which are produced by the oxidation of glucose and galactose.[36] Specifically, mucic acid is a dicarboxylic acid of considerable interest. Deoxydehydration reactions of such acids yield muconic acid or muconic acid diester (esterification product in acidic conditions), which are potential feedstock for the production of adipic acid, which is the basic monomer for the production of nylon 66. To bridge the gap between abundant sugars and value-added adipic acids, developing an efficient synthesis system is therefore in high demand.

Re-based catalysts show high potential for the conversion of sugar acids to adipic acid. The performance of homogeneous Re-based catalysts for mucic acid conversion is summarized in Table 3. Re-based catalysts with secondary and primary alcohols including 3-pentanol, 3-octanol and *n*-butanol are powerful systems to deoxygenate sugar acids. Owing to the excess use of alcohols, mixtures of carboxylic acids and esters are commonly obtained.[73] In detail, methyltrioxorhenium catalyzes mucic acid to muconic acid in 43–99% yields (Table 3, entries 1–3).[73–75] It has been found that Brønsted acids such as *para*-toluene sulfonic acid (TsOH) as a co-catalyst lead to a considerable reactivity increase for the deoxydehydration of mucic acid, and selectivity increases towards esterified products,[73] allowing for methyltrioxorhenium loadings as low as 0.5 mol%. This is mainly attributed to the assistance of the acid additive in olefin extrusion *via* Re diolate intermediate protonation.[76,77] Similarly, other Re compounds including $Cp^{tt}ReO_3$ and $L^4Re(CO)_3$ also have high catalytic activity for this reaction, leading to 75% and 46% yield of muconates (Table 3, entries 4 and 5). The experiment in Table 3, entry 6 shows that Re_2O_7 catalyzes deoxydehydration of mucic acid in 3-pentanol with high reaction rates. In moist environments, Re_2O_7 is transformed to $HReO_4$, which promotes the esterification and olefin extrusion steps in the deoxydehydration reaction. Thus, employing $HReO_4$ as a sole catalyst gives 62% and 71% yield of olefin with *n*-butanol as the solvent (Table 3, entries 8 and 9). Furthermore, Zhang *et al.* found that tuning the Lewis or Brønsted acidity of the reaction system is an efficient method to obtain high yields of carboxylic acids. For example, the methyltrioxorhenium system modified by pyridine can influence the selectivity of the reaction towards muconic acid with a yield of 74% by reducing the acidity of methyltrioxorhenium (Table 3, entry 3). It is noteworthy that coupling deoxydehydration reaction and heterogeneous hydrogenation catalysts such as Pt/C and Pd/C results in good yields of dibutyl adipate (Table 3, entries 2 and 9).[73,74]

According to the results shown above, the deoxydehydration reaction catalyzed by Re-based catalysts along with an alcohol reducing reagent can be regarded as the most efficient method for the removal of adjacent hydroxyl groups to form olefins. The advantages of employing an alcohol as both a reductant and solvent is that polyols or sugar acids have good solubility in alcohol. Additionally, the alcoholic reductants can be obtained *via* hydrogenation of alcohol oxidation products (ketones or aldehydes).

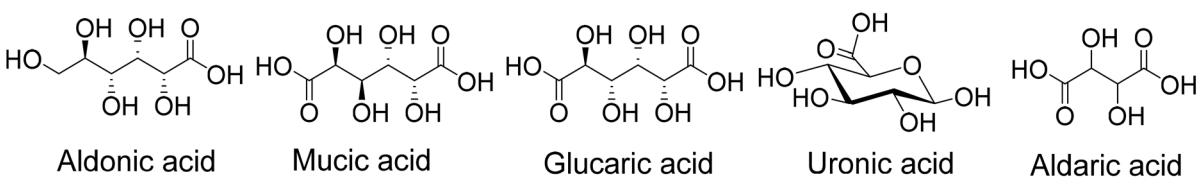

Fig. 4 The structure of typical sugar acids.

Table 3 Deoxydehydration reaction of mucic acid over Re-based catalysts

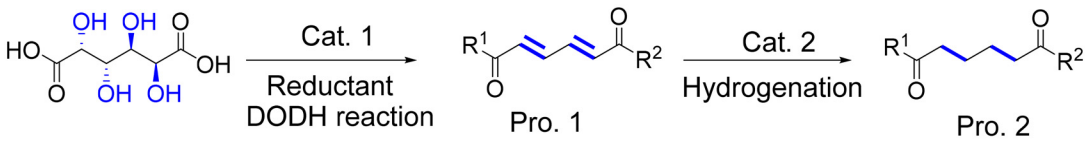

Entry	Cat. 1	Reductant	R^1	R^2	Yield/% Pro. 1	Condition	Cat. 2	Yield/% Pro. 2	Ref.
1	MTO	3-Pentanol	HO	HO	43	155 °C, 15 h, air	—	—	74
2	MTO	3-Pentanol	HO/OCH(C_2H_5)$_2$	OCH(C_2H_5)$_2$	99	120/160 °C, 12/12 h, air	Pt/C	99	73
3	MTO	3-Pentanol	HO	HO	74	120 °C, 24 h, N_2	—	—	75
4	Cp^{tt}ReO_3	3-Pentanol	HO/OCH(C_2H_5)$_2$	OCH(C_2H_5)$_2$	75	120 °C, 12 h, N_2	—	—	61
5	L^{4}Re(CO)$_3$	3-Octanol	HO/OC_8H_{17}	OC_8H_{17}	46	180 °C, 6 h, air	—	—	60
6	Re_2O_7	*n*BuOH	*n*BuO	*n*BuO	99	120 °C, 12 h, N_2	—	—	73
7	NH_4ReO_4	Indoline	*n*BuO	*n*BuO	57	150 °C, 24 h, N_2	—	—	64
8	$HReO_4$	*n*BuOH	*n*BuO	*n*BuO	71	170 °C, 7.5 h, N_2	—	—	74
9	$HReO_4$	*n*BuOH	*n*BuO	*n*BuO	62	170 °C/RT, 15/4 h, air/H_2	Pd/C	62	74

L^4 = 2,4-di-*tert*-butyl-6-(tetramethylethane-1,2-diamine)phenol; Cp^{tt} = 2,5-di-isopropyl-cyclopentadienyl; *n*BuO = *n*-butanol. MTO = methyltrioxorhenium.

With the aim to provide insights into the mechanism of the reaction (Fig. 5), the three main pathways are discussed. Toste *et al.* reasoned the reduction of the Re^{VII} center of methyltrioxorhenium to a Re^{V} specie, then followed by a condensation of a vicinal diol with the Re^{V} specie. The reaction, it has been assumed, proceeds *via* extrusion of olefin and catalyst regeneration (A in Fig. 5).[59] Abu-Omar *et al.* postulated route B in Fig. 5.[18] However, theoretical calculations suggested that their overall barriers are high. Therefore, Qu *et al.* provided route C in Fig. 5 as the most likely pathway of the reaction. According to density functional theory, the reduction of Re catalyst in a first step is more likely than the direct substrate condensation. Moreover, reduction with alcohol assisted by hydrogen transfer *via* the rhenium dihydroxy intermediate MeRe(OH)$_2$O is more stable than the dioxorhenium compound ($MeReO_2$). The olefin extrusion process is achieved by a concerted process of diolate cleavage to form the alkene.[78] Thus, alcohols apparently act as a shuttle to promote these hydrogen-transfer steps.

Tartaric acid, being a C_4 dicarboxylic acid ($C_4H_6O_6$), can be obtained from wine fermentation and oxidation of glucose,[79] which is extensively utilized in the pharmaceutical and cosmetic industries. Similar with deoxydehydration of mucic acid

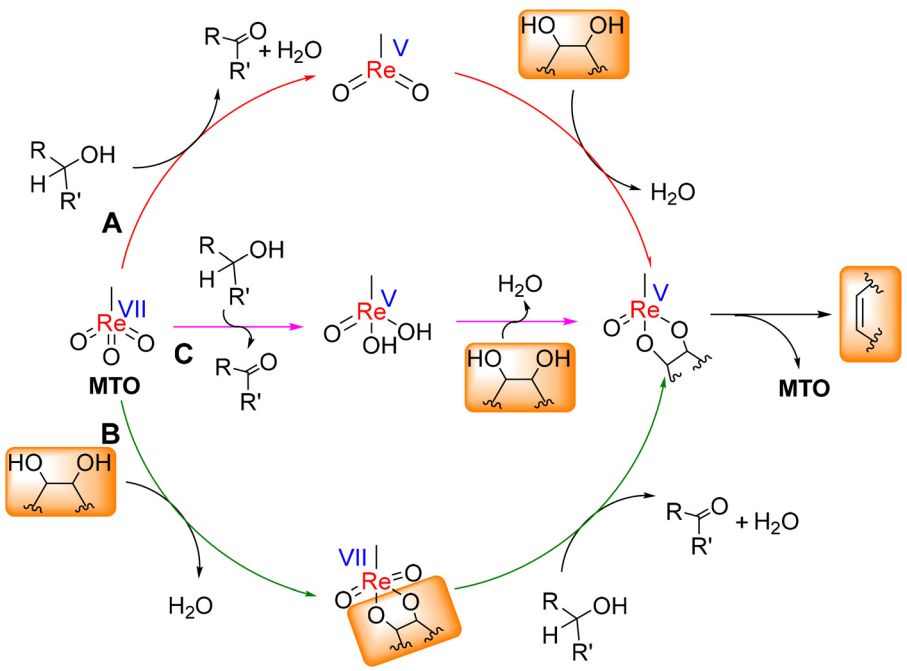

Fig. 5 Proposed mechanism C and alternative mechanisms A and B for deoxydehydration reaction of diols over MTO catalysts with alcohol reductants[78] (MTO: methyltrioxorhenium).

Table 4 Deoxydehydration reaction of tartaric acid over homogeneous Re-based catalysts

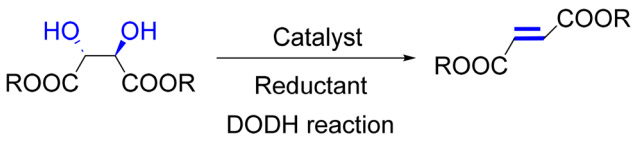

Entry	Catalyst	R	Reductant	Yield	Condition	Ref.
1	MTO	C_2H_5	Na_2SO_3	35%	150 °C, 84 h	63
2	$L^4Re(CO)_3$	H/C_8H_{17}	3-Octanol	81%	180 °C, 3 h	60
3	NH_4ReO_4	*n*-Bu	Indoline	78%	150 °C, 24 h	64
4	NH_4ReO_4	C_2H_5	Benzyl alcohol	95%	145 °C, 24 h	71
5	NH_4ReO_4	H	3-Pentanol	91%	120 °C, 24 h	75
6	$(Bu_4N)ReO_4$	C_2H_5	Na_2SO_3	10%	150 °C, 84 h	63

L^4 = 2,4-di-*tert*-butyl-6-(tetramethylethane-1,2-diamine)phenol.

to adipic acid, deoxydehydration of tartaric acid to maleic acid is regarded as the most efficient and promising method for the production of biopolymer precursors. Homogeneous Re-based catalysts such as methyltrioxorhenium, NBu_4ReO_4, NH_4ReO_4, and $L^4Re(CO)_3$ with a reducing agent enable transformation of tartaric acid or ester to maleic acid (Table 4). Specifically, the substrate (+)-diethyl L-tartrate can be converted to the *trans*-alkene, leading to 35% yield of diethyl fumarate with no *cis* products catalyzed by methyltrioxorhenium (Table 4, entry 1). However, the organometallic Re-based complexes $L^4Re(CO)_3$ vastly improve the yield reaching up to 81% with 3-octanol as the reductant at 180 °C (Table 4, entry 2).[60] NH_4ReO_4 has been applied with various reducing agents including indoline, benzyl alcohol, and 3-pentanol, to catalyze deoxydehydration reactions and yields >90% target products (Table 4, entries 3–5),[64,71] in contrast to the 10% diethyl fumarate yield for the NBu_4ReO_4 catalyst (Table 4, entry 6). Due to the versatile application of succinic acid in the synthesis of valuable C4 commodity chemicals and biodegradable polymers, it has been produced using tartaric acid as substrate *via* a two-step method. In detail, tartaric acid undergoes conversion to maleic acid with a notable yield of 91%, utilizing either methyltrioxorhenium-modified pyrimidine or NH_4ReO_4 catalysts (Table 4, entry 5), following further hydrogenation to succinic acid in 95% yield over Pt/C catalysts.[75]

Since γ-butyrolactone is a useful precursor for a multitude of polymers, the conversion of different lactone derivatives to γ-butyrolactone is an attractive reaction. With methyltrioxorhenium as the catalyst, conversion of D-erythronolactone to γ-butyrolactone is achieved at 155 °C in argon within 2.5 h and utilizes 3-pentanol as both the solvent and reductant. The subsequent hydrogenation is also achieved with the Pd/C catalyst (Fig. 6).[74] It is noteworthy that the final product γ-butyrolactone is the key precursor for the production of γ-hydroxybutanoic acid and γ-aminobutanoic acid through ring-opening reactions.

2.2 Conversion of lignin

Lignin, the second main component in lignocellulosic biomass, is considered as the only abundant source of aromatics in nature,[80,81] and regarded as a potential feedstock for aromatic bio-fuels and bio-chemicals.[10,81–83] However, its intrinsic recalcitrant nature and complex structure has so far made it more difficult to convert into fuels and aromatics with additional value. Model compounds of lignin, featuring typical and well-known structural bonds such as β-O-4, α-O-4, 4-O-5, β-1, β-β, and α-1, are frequently chosen as starting materials for the conversion processes. This choice mirrors the depolymerization of actual lignin, facilitating the study of its realistic breakdown.[84,85]

The organorhenium compounds methyltrioxorhenium and Re_2O_7 were employed as catalysts for the deconstruction of lignin model compounds containing β-O-4, and α-1 bonds through oxidations, redox-neutral reactions, and hydrogenation reactions (Fig. 7). The oxidation of lignin model compound catalyzed by methyltrioxorhenium/H_2O_2 has been the first attempt in disintegrating lignin.[86,87] When using the monomer vanillyl alcohol as the substrate, the oxidation products including vanillin and 4-hydroxy-3-methoxybenzoic acid

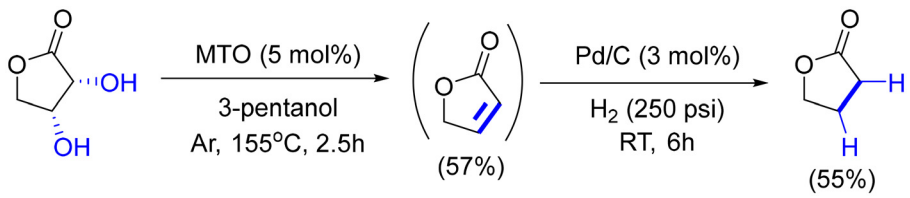

Fig. 6 Conversion of D-erythronolactone to γ-butyrolactone *via* deoxydehydration and hydrogenation reactions with methyltrioxorhenium as the catalyst[74] (MTO: methyltrioxorhenium).

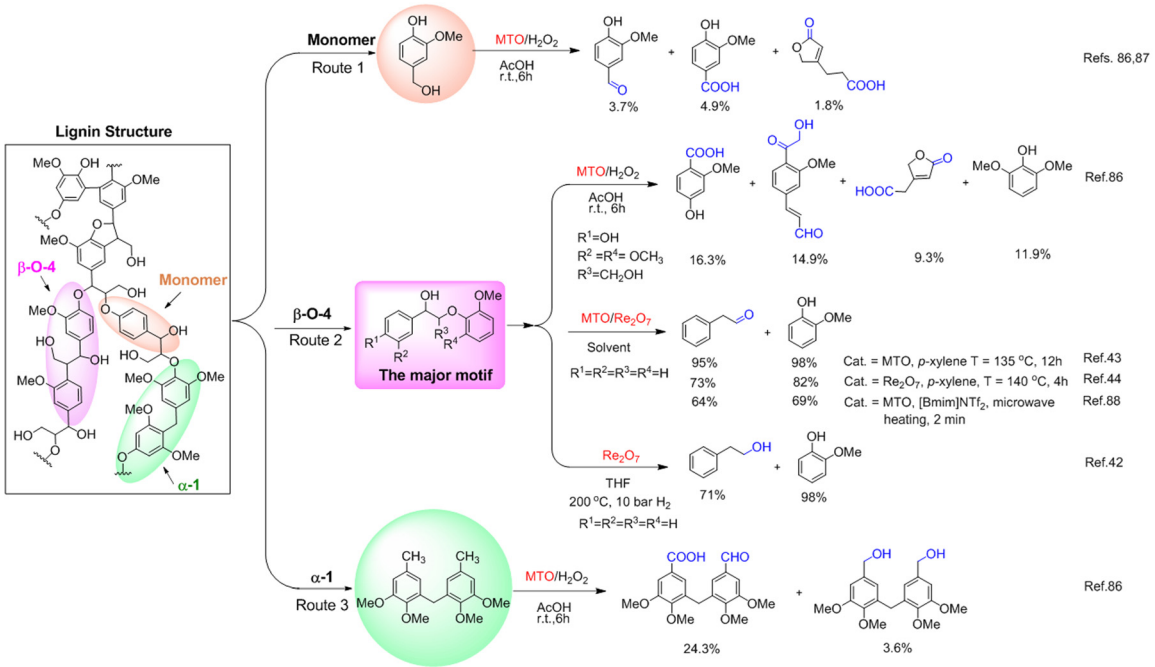

Fig. 7 Lignin model compounds catalyzed by Re-based compounds (MTO: methyltrioxorhenium).

are formed as major products in 3.7% and 4.9% yield (Fig. 7, Route 1). The β-O-4 patterns, being the major linkages, are further oxidized in the same catalytic system of methyltrioxorhenium/H_2O_2, leading to 40.5% carboxylic acid derivatives.[86] Additionally, an α-1 model compound has been modified *via* oxidation of side functional groups, and the C–C bond was maintained due to its high bonding energy. Interestingly, real lignin including spruce kraft lignin, hydrolytic sugar cane lignin and hardwood organosolv lignin can be degraded by using methyltrioxorhenium/H_2O_2. ^{31}P NMR has been employed to determine the amount of the different unstable OH groups. After methyltrioxorhenium oxidation degradation, high amounts of carboxylic acid moieties are obtained with low contents in aliphatic and condensed OH groups, indicating that methyltrioxorhenium is also highly efficient in oxidative depolymerization of real lignin.

Apart from the oxidation process, hydrogenolysis of such segments catalyzed by Re_2O_7 has been developed in the tetrahydrofuran and under 1 MPa H_2, affording 71% yield of phenylethyl alcohol and 98% yield of guaiacol.[42] In contrast, other metal oxide catalysts (WO_3, MoO_3, Fe_2O_3, CeO_2) show negligible activity in converting the same substrate.[42] When using pinewood as the feedstock, 19% yield of lignin oil is obtained at 200 °C and 3 MPa H_2 pressure within 8 h. Interestingly, the distribution of monomer products is similar to that obtained from isolated lignin.[42] Using pinewood lignin as the reactant, 76 wt% liquid oil with phenol compounds as the main products is obtained after 8 h of reaction at 200 °C, at 3 MPa H_2.[42] After characterization, the Re_2O_7 species in aromatic solvents shows Lewis-acidic properties for the cleavage of β-O-4 bonds in lignin.[44]

Since no additional H and O agents were present in the redox neutral process, it is regarded as the most promising approach for the depolymerization of lignin *via* C–O bond cleavage of β-O-4 groups. Notably, with methyltrioxorhenium as the catalyst, the redox neutral process of 2-(2-methoxyphenoxy)-1-phenylethan-1-ol yields 95% of phenylacetaldehyde and 98% of guaiacol.[43] Although this catalytic system is homogeneous, methyltrioxorhenium can be reused at least five times without loss of activity through removing all volatiles *in vacuo*. The catalytic system has been extended to the aliphatic ether 2-phenoxycyclohexan-1-ol, conducted at 155 °C for 45 h in *p*-xylene solvent. This reaction yields 18% ketone, 26% phenol, and 15% dehydration products.

Methyltrioxorhenium is also active as a catalyst for the cleavage of β-O-4 bonds in model compounds and real lignin in the ionic liquid of 1-butyl-3-methylimidazolium bis(trifluoromethylsulfonyl)imide (B[mim]NTf_2).[88] When the reaction medium is treated with microwave irradiation for 2 min at 240 W and 180 °C, 64% yield of guaiacol and 98% yield of phenylacetaldehyde (Fig. 7, Route 2) are obtained. Microwave irradiation shortens the reaction time to 2 min, which might be attributed to the enhancement of the catalyst's activity and the substrate's solubility under electromagnetic radiation. Notably, organosolv birch lignin catalyzed by methyltrioxorhenium in [Bmim]NTf_2 for 2 min at 180 °C produces 34.2% yield of low molecular weight lignin oil, mainly consisting of aromatic monomers.[88] Besides methyltrioxorhenium, Re_2O_7 catalyzes the deconstruction of β-O-4 model compounds through a redox neutral reaction, leading to 73% yield of phenylacetaldehyde and 82% yield of guaiacol (Fig. 7, Route 2).[44] In addition, modification of an α-1 model compound catalyzed

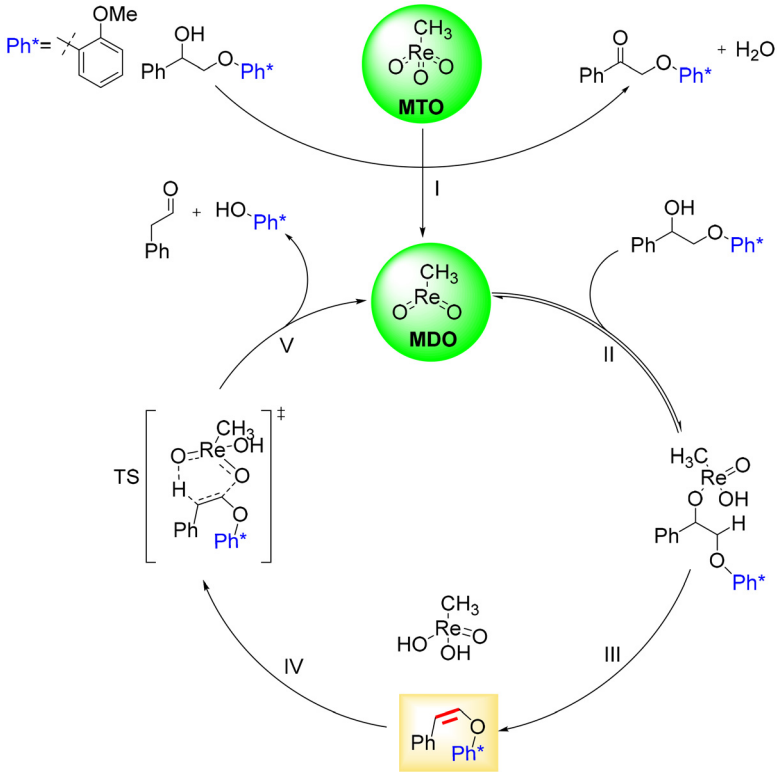

Fig. 8 The mechanistic pathway of Re-catalyzed cleavage of lignin β-O-4 model compound (MTO: methyltrioxorhenium; MDO: methyldioxorhenium).

by methyltrioxorhenium with H_2O_2 is achieved at room temperature although C–C bonds remain in the final products (Fig. 7, Route 3).[86]

The major pathway for the cleavage of the C–O bond in lignin β-O-4 model compounds proceeds as an initial excitation by dehydration of the β-O-4 model compound to the alkenyl ether intermediate, then the cleavage of C–O bond with organorhenium catalysts (Fig. 8). This mechanism diverges from previous redox-neutral processes by involving the cleavage of β-O-4 bonds through α-ketone formation *via* dehydrogenation reactions.[89] Isotope labeling experiments and density functional theory calculations indicate the reduction of Re^{VII} to Re^{V} by the lignin model compound. This reduction suggests that methylrhenium dioxide is responsible for the cleavage of C–O bonds. According to the control experiments and density functional theory calculations, the different reaction mechanism should be attributed to the O shift of the substrate OH group and methyltrioxorhenium, which is typical of Re catalysts in lignin depolymerization reactions.

3. Heterogeneous Re-based catalysts for biomass conversion

3.1 Conversion of (hemi)cellulose

Inspired by the works in the conversion of cellulose to polyols and glycols,[90–92] extensive works have been conducted on the transformation of cellulosic biomass over heterogeneous Re-based catalysts (Fig. 9, Route 1). Liu *et al.* employed Re oxides to modify Ir catalysts for cellulose conversion. Over the binary Ir–ReO_x/SiO_2 and HZSM-5 catalysts, the hydrolysis and hydrogenation–hydrogenolysis reactions were coupled to yield 83% of *n*-hexane in a biphasic reaction system of *n*-dodecane and water.[93] However, the main product shifted to hexanols over the same Ir–ReO_x/SiO_2 catalyst after modifying the reaction conditions to 140 °C for 24 h at 10 MPa H_2. Under these reaction conditions, cellulose is depolymerized to glucose by the mechanocatalytic method. Next, using Ir–ReO_x/SiO_2 catalysts, the glucose is hydrogenated to produce sorbitol. Finally, hydrogenolysis of sorbitol into hexanols is achieved by the synergy of Ir–ReO_x/SiO_2 and H_2SO_4, and hexane is obtained as the final product (Fig. 9, Route 1).[94] In subsequent work, the same group employed hemicellulose as the feedstock, and also obtained *n*-pentane, pentanols or xylitol by simply adjusting the reaction conditions over the same Ir–ReO_x/SiO_2 catalyst combined with acids. According to extensive characterization studies, hydroxorhenium sites (Re–OH) were found to be the active sites of Ir–ReO_x/SiO_2 for the C–O bond hydrogenolysis in carbohydrates.[33]

Carbohydrates such as glucose and fructose are the main components of biomass and have been selected as probe molecules for catalytic conversions. When using glucose as the feedstock, over the Ir–ReO_x/SiO_2 catalyst, around 95% of *n*-hexane is obtained after 84 h of reaction at 140 °C in the

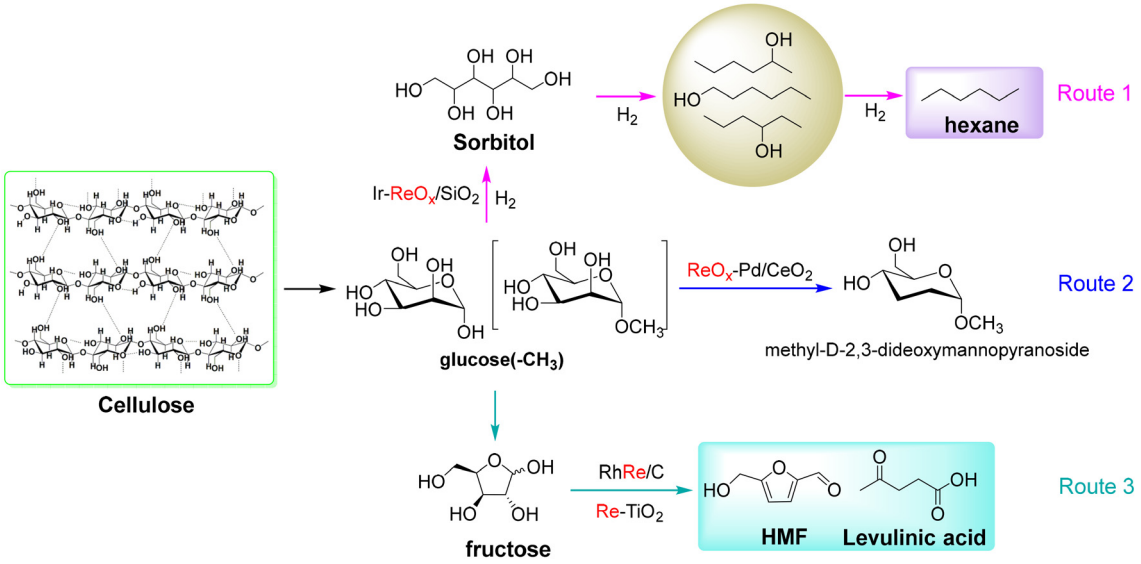

Fig. 9 Catalytic conversion of cellulosic biomass into chemicals over Re-based catalysts.

presence of 8 MPa H_2, much higher than the cellulose conversion counterpart (Fig. 9, Route 1).[32] During the conversion of sugars, the same group found that ReO_x–Pd/CeO_2 catalysts selectively transform sugars into chiral polyols with retention of the intrinsic configuration (Fig. 9, Route 2). Specifically, employing methyl glycosides as the feedstock, vicinal OH groups can be selectively removed *via* the deoxydehydration–hydrogenation reaction without breaking of the C–C bonds. Under typical reaction conditions of 140 °C for 24 h with a H_2 pressure of 8 MPa, the methyl-D-2,3-dideoxy-mannopyranoside yield surpasses 90%, serving as an effective reaction process for producing stereostructure chemicals. Additionally, this product is an ideal feedstock for producing chiral polyol building blocks and diols *via* hydrolysis and/or hydrogenation reactions.[95]

Apart from these deoxydehydration and hydrodeoxygenation reactions, Re-based catalysts were also employed for carbohydrate dehydration due to its specific acidic properties. By adjusting reaction conditions, different carbohydrate sources can be transformed into ethyl levulinate, 5-ethoxymethylfurfural, 5-hydroxymethylfurfural and levulinic acid over a $HReO_4$ catalyst.[96] To solve the recycling issues, Re species were incorporated into metal catalysts for sugar conversions. Chia *et al.* synthesized RhRe/C catalysts for the dehydration of fructose to 5-hydroxymethylfurfural, and confirmed the acidic properties of Re species in liquid water.[97] Recently, Avramescu *et al.* loaded Re onto TiO_2 for carbohydrate conversion. The balanced Brønsted and Lewis acid sites catalyze the glucose isomerization and dehydration reactions, and yield 57% of levulinic acid over 10% Re–TiO_2 catalyst in four catalytic cycles (Fig. 9, Route 3).[98]

3.2 Conversion of lignin

Due to the high activity of methyltrioxorhenium(VII) in catalyzing the oxidation of aromatic derivatives, immobilized methyltrioxorhenium was developed for the transformation of lignin utilizing polymeric support, such as poly(4-vinylpyridine and polystyrene). Employing immobilized methyltrioxorhenium as the catalyst and H_2O_2 as the oxidant agent, the lignin derived from sugarcane and red spruce decomposes at room temperature into soluble lignin fragments with higher amounts of carboxylic acid groups.[87]

To make full use of the ReO_x sites, they are loaded on different supports for depolymerization of lignin model compounds and real lignin to aromatics and cycloalkanes through hydrogenation and hydrodeoxygenation reactions. Currently, the hydrogenation and hydrodeoxygenation reactions of lignin concentrate on lignin monomers including guaiacol, phenol, anisole, dimers containing β-O-4, 5-5 model compounds, and real lignin. Controlled selective hydrogenation of lignin model compounds still remains a challenge due to some side reactions. Selecting guaiacol as an example, guaiacol can be converted through several pathways, as shown in Fig. 10: guaiacol can be demethoxylated to phenol, and further hydrogenolyzed to benzene. The conversion of guaiacol to anisole through hydrogenolysis is achieved by alkylation/transalkylation of anisole to methyl anisole. The final products toluene and methyl cyclohexane are produced through hydrogenation of cresol. The whole reaction system is rather complicated, bearing a huge challenge to achieve a catalyst for improving the selectivity for the target products. Thus, Re-based compounds could be ideal candidates for the controlled hydrogenation reaction owing to the multitude of their accessible valences. For instance, Re supported on active carbon (AC) has been carburized under different temperatures between 500 °C and 700 °C under H_2/C_2H_4 with the ratio of 75 : 25, forming ReC at 700 °C, Re_xC at 650 °C, and a mixture of Re metal, oxide, oxycarbide and carbide between 500 °C and 600 °C. Phenol as the main product is obtained for all the catalysts, while at high conversion (>80%) phenol starts to further

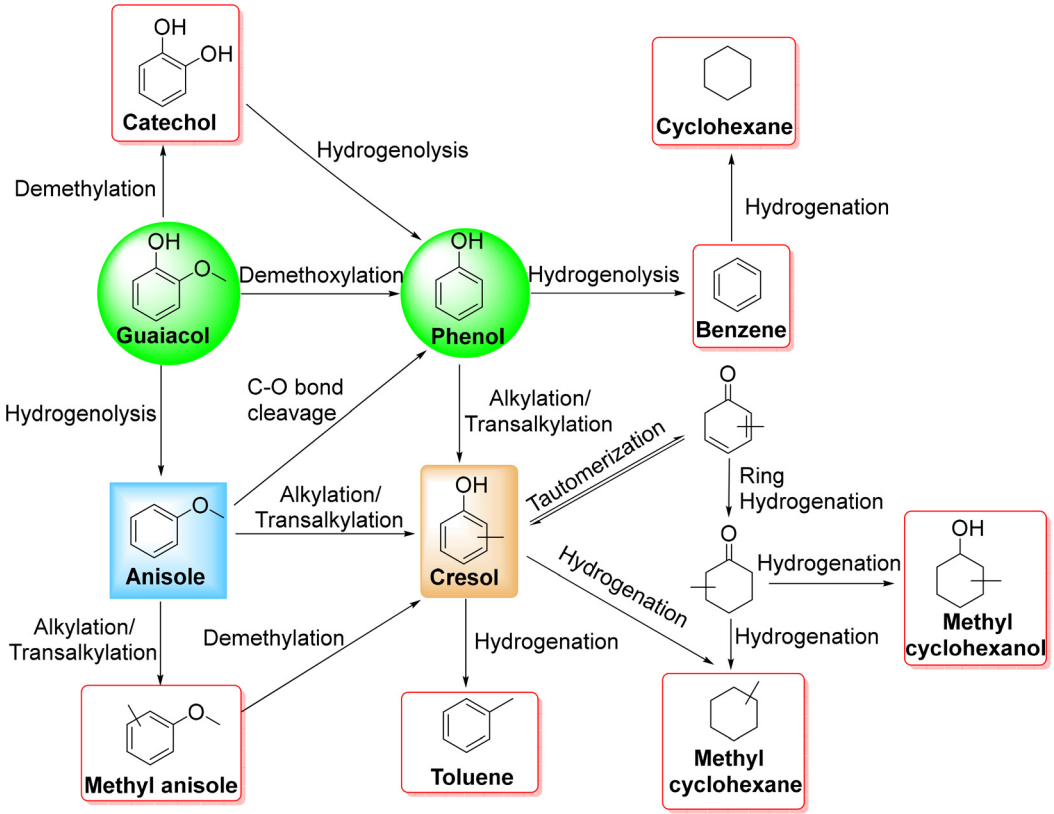

Fig. 10 The possible pathways for guaiacol, phenol and cresol conversion.

convert into benzene. Utilizing only Re_xC as the predominant active phase, a benzene yield of 51% is achieved, attributed to the suppression of phenol hydrogenolysis into benzene.[99] Later, Re-based bimetallic catalysts were developed for improving the catalytic activity. For instance, $FeReO_x/ZrO_2$ has been prepared by the incipient wetness co-impregnation method, and used for hydrodeoxygenation of phenolics such as guaiacol, *m*-cresol and anisole.[100] Compared to Fe/H-Beta(38), $FeReO_x/ZrO_2$ shows clear enhancement in terms of performance for hydrodeoxygenation of phenolics. The yield of BTX mixture products (BTX = benzene, toluene and xylenes) is almost two times higher than in the case of Fe/H-Beta(38) at 350 °C and 0.1 MPa H_2. The variations in performance can be attributed to the finely balanced acidity resulting from both the presence of Re oxide and the Zr support, leading to enhanced dehydration efficiency. A range of catalysts, comprising a base-metal (Re, Ga, Ni, and Co) combined with reducible metal oxides (Mo and V), were developed for the hydrodeoxygenation of anisole into benzene/toluene products.[101] Among these catalysts, $Re–MoO_x/TiO_2$ and $Re–VO_x/TiO_2$ exhibit notably high catalytic activity in breaking C–O bonds to produce benzene and toluene products at 300 °C and 3 MPa H_2. The catalytic performance of $Re–MoO_x/TiO_2$ primarily stems from exposed Mo^{5+} sites, whereas that of $Re–VO_x/TiO_2$ is governed by Re^{4+} sites. Control experiments and characterization studies have led to the conclusion that despite the Mo^{5+} sites having the highest intrinsic activity, the presence of Re as a specific type of active site in an appropriate amount is required to enhance benzene/toluene production. Besides the abovementioned study, hydrodeoxygenation of monomers to cycloalkanes is regarded as a direct way to obtain alkanes. When using cresol, anisole, and phenolic compounds as substrates, the inclusion of Re causes the bulk surface of Ni/Cu/Fe to fragment into smaller ensembles, leading to a reduction in the electron density of the metals' d-band through both geometric and electronic influence, resulting in a high activity in the hydrodeoxygenation of lignin monomers without the hydrogenolysis of C–C bonds of the products, affording high alkane yields.[100,102–104]

Re-based catalysts also have outstanding performance for the selective cleavage of C–O bonds in lignin β-O-4, α-O-4, β-1, α-5, and 5-5 model compounds and real lignin through hydrogen and a hydrogen donating solvent, as shown in Fig. 11. According to the results of model compounds' hydrogenation, different phenols and alkanes can be synthesized selectively. Zhang *et al.* found ReO_x/AC catalyzes the selective cleavage of C–O bonds of lignin β-O-4 model compounds delivering ethylbenzene and guaiacol as major products in 81.6% and 83.0% yield through a H-transfer reaction at 200 °C and 0.7 MPa N_2 (Fig. 11a).[41] ^{i}PrOH has been utilized as both the solvent and hydrogen donor for reductive cleavage of the ether bonds in this case. The reaction involves dehydration, dehydrogenation, and direct hydrogenolysis, with dehydration to vinyl ether intermediates being the major route.[41] Furthermore, the ReO_x/

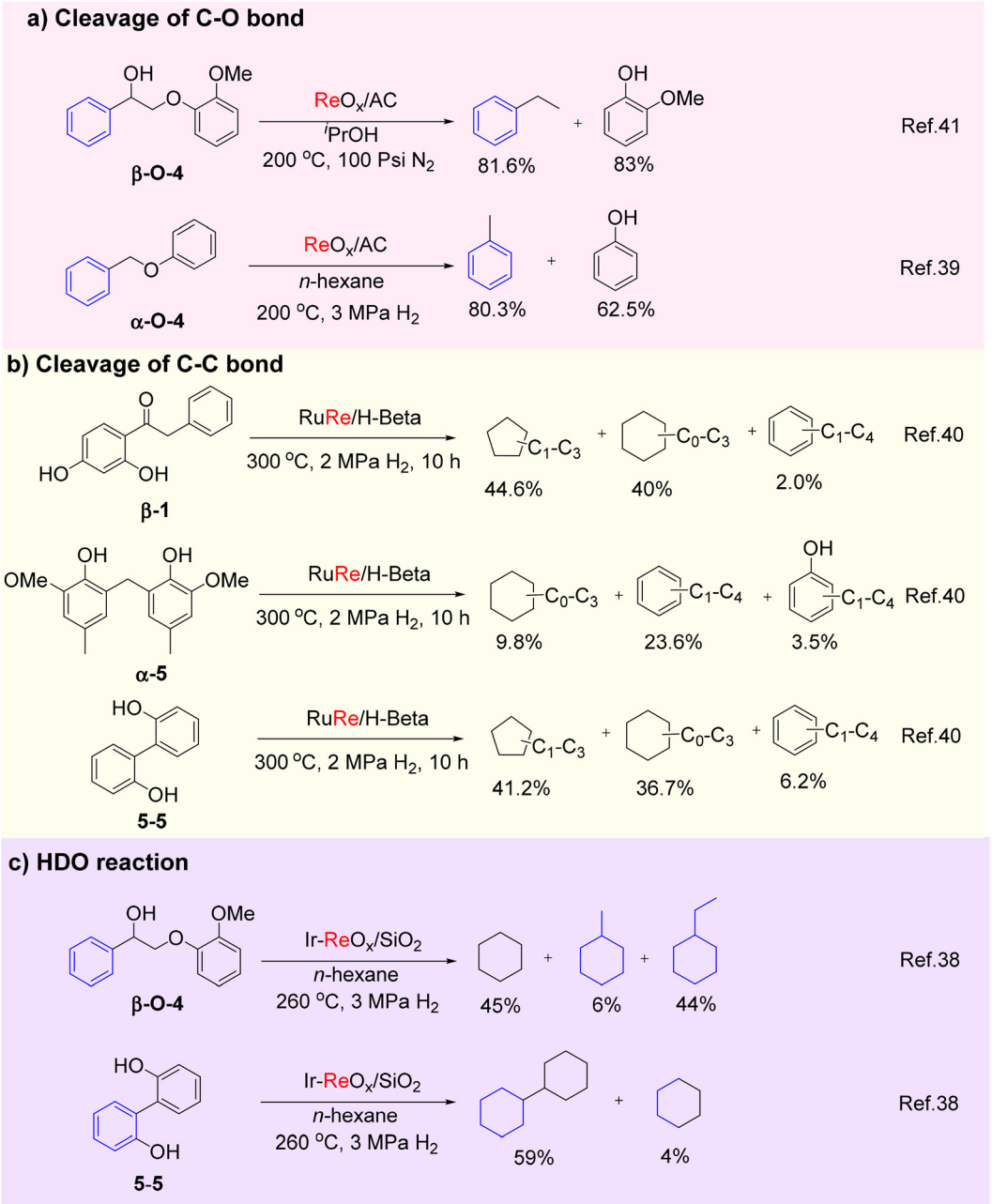

Fig. 11 Cleavage of C–O/C–C bonds in lignin model compounds over Re-based catalysts.

AC catalyst can also be utilized for the deconstruction α-O-4 model compounds, leading to 80.3% yield of toluene and 62.5% yield of phenol at 200 °C and 3 MPa H_2.[39] Re 4f XPS showed the conversion of ReO_x species into low valence states during catalysis. However, the species is easily oxidized with air. Lignin linkages involving C–C bonds are regarded as the most stable bonds due to their high bond dissociation energies.[105] In further research progress, a RuRe alloy was developed for the deconstruction of β-1, α-5, and 5-5 model compounds, affording a mixture of alkanes and aromatics in 36.9–86.6% carbon yields at 300 °C and 2 MPa H_2.[40] Furthermore, both kraft lignin and alkaline lignin underwent degradation, involving the breaking of C–C and C–O bonds, ultimately yielding monocyclic products at the maximum theoretical yield based on the cleavage of C–O bonds in real lignin.

The hydrodeoxygenation degradation of lignin is another effective way for the production of alkanes, which is the most direct protocol for the production of fuels. For instance, an Ir–ReO_x/SiO_2 catalyst was prepared by the wetness impregnation method, and used for the one-pot conversion of various compounds modeling lignin structures and three kinds of lignin (enzymolysis lignin, organosolv poplar lignin and commercial alkaline lignin) into alkanes.[38] Various lignin models includ-

ing β-O-4 and 5-5 were converted to cyclohexane in 95% and 63% carbon yield as well (Fig. 11c).

Compared to model compounds, lignin causes more problems due to lower solubility and more complicated structure, when degradation to phenolics is to be achieved (Fig. 12). Depolymerization of lignin is divided into two processes: oxidation and hydrogenolysis reactions. In the oxidative depolymerization process, the challenge lies in controlling bond cleavage and catalyst inefficiencies. NiO–Re_2O_7/GO has been developed to catalyze fractionated bagasse lignin into 28.4% yield of phenolics, producing guaiacol as the main product, which is higher compared to the conversion without incorporating Re into NiO/GO (23.7%).[106] This catalyst can be reused five times. The significant improvement observed can be attributed to the capability of Re to enhance both metal dispersion properties and selectivity in ether bond cleavage within lignin.

Hydrogenolysis stands as another highly effective method for lignin depolymerization, involving either the addition of H_2 or hydrogen-transfer reactions. Using ReO_x/AC with ^{i}PrOH as both the solvent and H-source, catalysis of organosolv poplar lignin and organosolv wheat lignin yields monophenolics at 11.4 wt% and 5.3 wt%, respectively, at 200 °C and 100 psi N_2. Incorporating noble metals significantly enhances selectivity toward aromatics under H_2 atmosphere. For example, PtRe/TiO_2 catalysts show activity in β-O-4 bond cracking in extracted birch lignin. After 12 h of reaction at 240 °C, a notable 18.7 wt% monophenol yield, including 7.5 wt% of 4-propylsyringol, is achieved using isopropanol as an *in situ* hydrogen donor.[107]

Apart from H-transfer reactions, depolymerization by H_2 addition could favor the degradation of lignin into small molecules. ReS_2/Al_2O_3 catalysts were obtained after sulfidation with dimethyl disulfide in the presence of H_2, and they convert lignin into 21.5 wt% monocyclic product with 72.4% lower char yield due to the high oxophilicity. The metal-like behavior of Re sulfide stabilizes the depolymerized lignin fragments.[108] By means of the precipitation–deposition and impregnation procedures, magnetic nanoparticles of Fe_3O_4@SiO_2@Re can be synthesized for the fragmentation of lignin into aromatics. Over the recyclable catalyst, the Re species were found to catalyze both C–C and C–O bonds in the presence of H_2 at 180 °C.[109] Different characterization studies of this catalyst showed that Re was not reduced to the metallic state and weakly acidic Brønsted-type centers were created. Furthermore, Fe_3O_4@Nb_2O_5@Co@Re was developed *via* a multistep process and catalyzed lignin to lignin fragments. Compared to a maximal 40% yield in water-soluble fragments over monometallic Fe_3O_4@Nb_2O_5@Co, the addition of Re improved the catalytic activity and up to 85% yield of light fragments was achieved due to the synergetic effect between Co and Re metals.[110] In subsequent advancements, bimetallic ReMo@zeolitic imidazolate framework (ZIF) catalysts have been able to crack kraft lignin, yielding 92% of monophenols in the liquid products. This outcome aligns with the observed synergistic effect between ReO_x and MoO_x in promoting phenol conversions.[111,112] Similarly, in the presence of Ni over NbO_x, kraft lignin is catalytically transformed with 96.7 wt% yield of oil after 3 h of reaction at 330 °C over 5Ni–5Re/Nb_2O_5 catalysts.[113]

In reductive approaches, an Ir–ReO_x/SiO_2 catalyst with both acidic and basic sites was used for one-pot conversion of lignin, resulting in 44.3 wt% yield of naphthenes from organosolv lignin at 260 °C at 4 MPa H_2. This high performance is attributed to a synergistic effect between Ir and ReO_x in Ir–ReO_x/SiO_2. During the mechanistic study, ReO_x and Ir species were proved to be responsible for C–O cleavage and hydrogenation of aromatic rings, respectively.[38]

Converting woody biomass, composed of cellulose, hemicellulose, and lignin, into value-added chemicals remains a considerable challenge, primarily due to the intricate structure and inherently resistant chemical composition of raw lignocellulosic biomass. Currently, pyrolysis and pretreatment processes are utilized to extract individual components from woody biomass for utilization. However, these methods require extensive energy input and incur high costs. The catalytic utilization of all three components simultaneously towards different chemicals offers the potential for maximum conversion efficiency. Designing a robust and multifunctional catalyst is crucial for this purpose. Li *et al.* have developed Ni–ReO_x/CeO_2, which catalyzes the transformation of woody biomass to both aromatics and alkanes, as shown in Fig. 13. Under mild reaction conditions, Ni–ReO_x/CeO_2 achieves an 88.4% yield of lignin oil from woody biomass. Conversely, under harsh conditions, it converts the same substrate into alkanes. These results demonstrate that the catalyst can operate in two modes: first, preserving cellulose in a lignin-first reaction protocol, and second, converting the entire substrate into alkanes with 43.8% carbon yield.[45] Additionally, the catalyst possesses magnetic properties, facilitating easy separ-

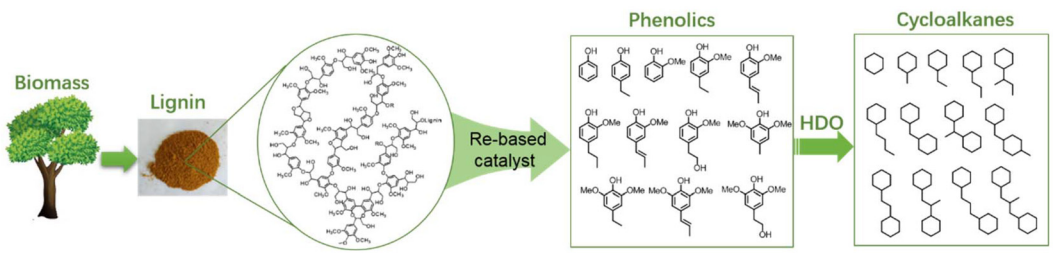

Fig. 12 Depolymerization of lignin to phenolics over Re-based catalysts.

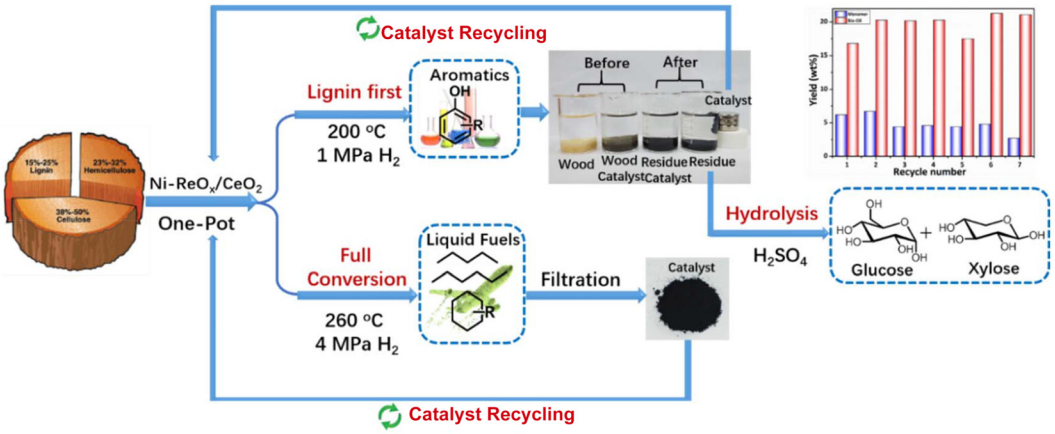

Fig. 13 Conversion of woody biomass to aromatics and alkanes over Ni–ReO_x/CeO_2.[45]

ation and enabling its reuse for up to seven cycles. This protocol presents a clear advantage for cost-efficient production of aromatics and fuels, while bypassing the need for pretreatment processes.[45]

3.3 Conversion of platform chemicals

Besides applications in the upgrading of cellulosic biomass and lignin, Re-based catalysts have also been widely used in upgrading platform chemicals *via* hydrogenation, hydrogenolysis, hydrodeoxygenation and deoxydehydration reactions.

3.3.1 Direct hydrogenation of the C=C bonds. Similar to some precious metal catalysts, supported Re catalysts show high activity in C=C bond hydrogenation without affecting the aromatic rings or carboxylic groups. Over the ReO_x/TiO_2 catalyst with weak binding between metal oxide and support (Fig. 14), *trans*, *trans*-muconic acid can be selectively hydrogenated into adipic acid with >88% selectivity to dimethyl adipate after 5 h of reaction at 210 °C and a hydrogen pressure of 6.89 MPa.[114] By the atomic layer deposition method, methyltrioxorhenium can be introduced into the metal–organic framework of NU-1000. This material can be applied in ethene hydrogenation for at least 1 day.[115] Under these reaction conditions, a large number of reduced Re sites are formed, attributed to the improved hydrogenation activity in C=C bond conversions.

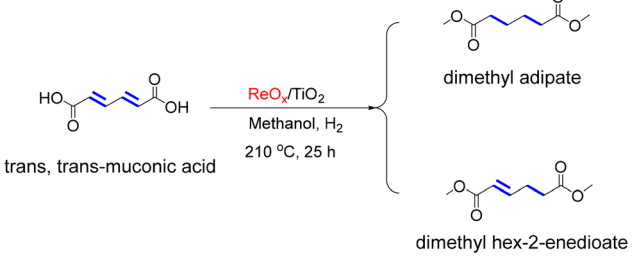

Fig. 14 Hydrogenation of muconic acid into different adipic acid esters in methanol over ReO_x/TiO_2 catalysts.[114]

3.3.2 Direct hydrogenation of the C=O bonds. In most cases, carboxylic acids or esters with C=O bonds are difficult to be hydrogenated due to the low electrophilicity of carbonyl carbon atoms.[116,117] Interestingly, Re based catalysts demonstrate high activity for C=O bond hydrogenation, especially in the presence of metal catalysts (Table 5).

During the transformation of C_6–C_{18} fatty acids to alcohols, ReO_x shows high selectivity for alcohols only under harsh reaction conditions.[118,119] In the presence of metals, the activity and product selectivity were greatly improved due to the synergistic effect between metal and ReO_x species.[120–123] In Fig. 15, among both monometallic and bimetallic catalysts, the Ni_1Re_1 catalyst demonstrates the highest TOF (turnover frequency), underscoring the pivotal contribution of Re species in bolstering catalytic activity. The H_2-TPD findings suggest that the introduction of Re species amplifies the catalyst's capability for hydrogen activation and dissociation, thereby generating a greater abundance of active hydrogen atoms crucial for the hydrogenation reaction. Moreover, the NiRe alloys promote fatty acid adsorption on the catalyst surface, favouring the conversion of fatty acids to alcohols. As a result, over the Ni_1Re_1 catalyst, fatty acid conversion surpasses 95% with >90% selectivity for fatty alcohols under mild conditions (150 °C and 4.0 MPa hydrogen).[124] Additionally, the presence of Re species enhances the rate of hydrodeoxygenation and shifts the product from *n*-heptadecane to *n*-octadecane for ethyl stearate conversions. Over the Ru–Re/TiO_2 catalyst, the ratio of *n*-octadecane/*n*-heptadecane reached 3.2 due to the newly formed weak acid sites of the catalyst.[125]

Hydrogenation of succinic acid into value-added chemicals is highly attractive but challenging over most metal catalysts.[126] In contrast, over ReO_x/C catalysts, γ-butyrolactone, the key intermediate for 1,4-butanediol production, is preferably formed, due to the weak activity of Re species for the ring-opening of γ-butyrolactone.[127,128] After introducing metal sites, the main product shifts to 1,4-butanediol due to the synergistic effect between metal and Re species.[129] Over Pd(Ru,

Table 5 Some typical reaction results for C=O bond hydrogenation over Re based catalysts

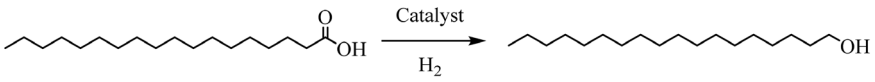

Entry	Catalysts	Reaction type	Solvent	T/°C	P/MPa	Time/h	Con./%	Sel./%	Ref.
1	Reduced Re_2O_7	Batch	Water–dioxane	265	24.5	23.5	71	60.5	118
2	ReO_x/TiO_2	Batch	Dodecane	220	2.0	—	80	88	119
3	Re–Pd/SiO_2	Batch	1,4-Dioxane	140	8.0	4	18	94	121
4	Ir–ReO_x/SiO_2	Batch	Cyclohexane	180	2.0	1	100	94	122
5	Pt–Re/TiO_2	Batch	Dodecane	130	2.0	5	62	83	123
6	Ni_1Re_1	Batch	Cyclohexane	150	4.0	5	99	94.5	124
	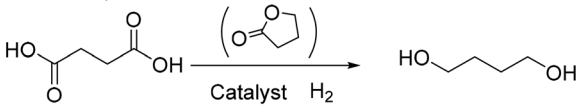								
7	Pd–Re/TiO_2	Batch	Water	160	15.0	48	100	83	129
8	Re–Ru/MC	Batch	1,4-Dioxane	200	8.0	7	100	71.2	130
9	Re–Pd	Batch	1,4-Dioxane	140	8.0	96	100	89	131
10	Re–Pt/C	Batch	Water	160	8.0	—	>99	80	132
	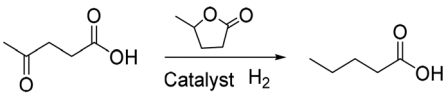								
11	ReO_x/ZrO_2 (SiO_2)	Batch	1,4-Dioxane	200	5.0	3	100	>90 (GVL)	138
12	Re–Ru–O/HZSM-5	Batch	—	230	4.0	4	—	65% yield valeric acid/esters	140
	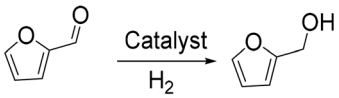								
13	$PdRe/Al_2O_3$	Fixed-bed reactor	—	150	0.1	—	10	66.7	142
14	ReO_x/SiO_2	Batch	Dodecane	200	4.0	4	10	70	143

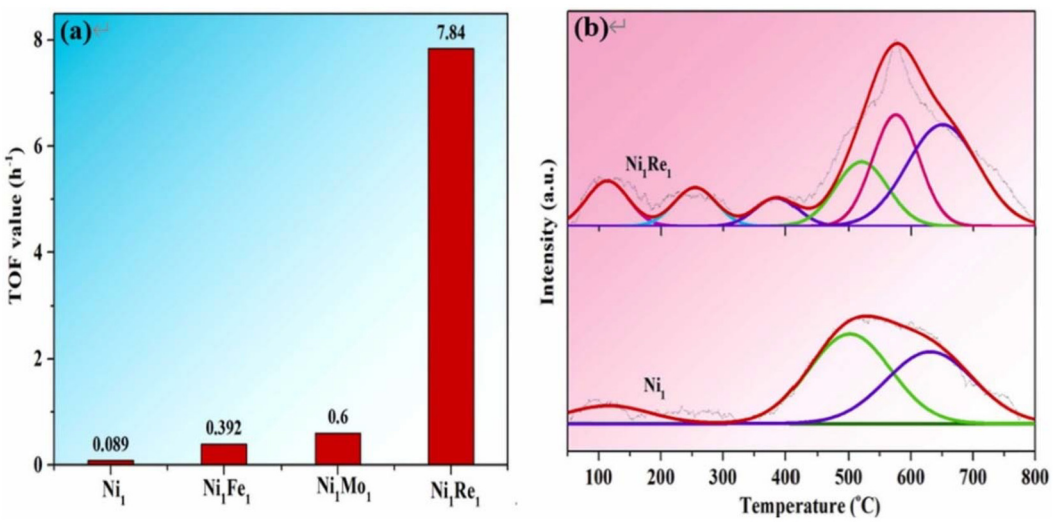

Fig. 15 (a) Comparison of TOF values over different reduced catalysts (0.1 g of fatty acid, 0.02 g of activated catalyst in 10 mL of cyclohexane solvent at 150 °C and 4.0 MPa hydrogen); (b) H_2-TPD profiles of the reduced Ni_1 and Ni_1Re_1 catalysts.[124]

Pt)–ReO_x catalysts, the succinic acid conversion reaches 100% with >70% 1,4-butanediol selectivity.[129–132] According to *in situ* characterization, metallic Re and Re^{3+} species are present, which interact with high coordination metal species to bifunctional sites for the selective hydrogenolysis of the intermediate of γ-butyrolactone to 1,4-butanediol.[133–135] In detail, over a Pd–ReO_x/TiO_2 catalyst with active Pd–ReO_x interfaces, the activation of γ-butyrolactone occurs on protonated Re species bound to Pd atoms, forming an intermediate with both the carbonyl group and the oxygen in the cycle, which

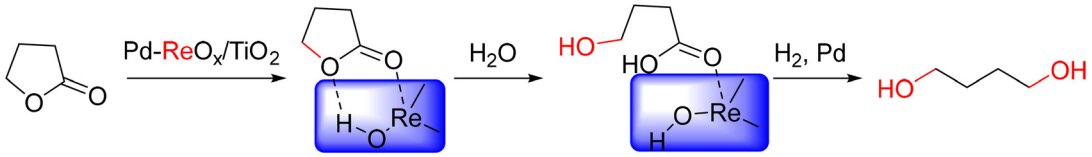

Fig. 16 Schematic reaction pathway for the conversion of γ-butyrolactone to 1,4-butanediol.[133]

are then transformed into an ester intermediate and further hydrogenated over Pd^0 sites to yield 1,4-butanediol (Fig. 16).[133]

As one of the ten high-value biomass-derived compounds from lignocellulosic biomass, levulinic acid is employed for producing a large number of commodity chemicals.[136,137] Over Re oxides supported on ZrO_2 and SiO_2, the γ-valerolactone selectivity exceeds 90% regardless of the support used, demonstrating the bifunctional properties of ReO_x species under reaction conditions.[138] Over a RuRe/C catalyst, 1,4-pentanediol is preferably produced with selectivity up to 75% at 130 °C and 50 bar H_2. According to the *in situ* FT-IR spectroscopy results, the presence of Re species promoted the adsorption of the reactant and intermediates, and then facilitated the ring-opening hydrogenation of γ-valerolactone to 1,4-pentanediol.[139] The product changes to methyl valerate and valeric acid when using neat methyl levulinate as the feedstock over Re–Ru–O/HZSM-5 catalysts. The authors propose that the ReO_x species catalyzes the conversion of methyl levulinate to γ-valerolactone, the acidic HZSM-5 promotes the ring-opening of γ-valerolactone, and the ReO_x modified Ru hydrogenates the intermediate to valeric compounds.[140] Similarly, ethyl levulinate is transformed into ethyl-4-ethoxy pentanoate with 83% yield at 160 °C for 2 h under a pressure of 1 MPa H_2 over $NiReO_x$/Beta catalysts. The presence of ReO_x increases the dispersion and reducibility of NiO over the support of Beta zeolite, affording large amounts of Lewis acid sites and Brønsted acid sites for ethyl levulinate conversions.[141]

Re based catalysts have also been used for other C=O bond hydrogenations in biomass conversions. For instance, PdRe/Al_2O_3 catalysts show greater furfuryl alcohol selectivity and activity than Pd/Al_2O_3 catalysts for furfural conversions due to the intimate contact of Re clusters with the surface Pd particles.[142] At a higher reaction temperature of 200 °C, furfuryl alcohol is produced over ReO_x/SiO_2 catalysts, and then shifted to a mixture of furfuryl alcohol and 2-methyl furan, when the reaction time is extended, confirming the high hydrogenation activity of partial reduced ReO_x species.[143]

3.3.3 Direct hydrogenation of C–OH bonds. Different from most metal oxides or metals, the Re species show unique selectivity in tailoring the –OH group of biomass-derived chemicals such as glycerol, erythritol and carbohydrates *via* the hydrogenation, hydrodeoxygenation and deoxydehydration reactions.[144] 1,3-Propanediol is a very promising target product for glycerol conversion because of the versatile application of 1,3-propanediol and the structural similarities between reactant and product.[145] However, hydrogenolysis of glycerol to 1,3-propanediol is very challenging because this reaction needs to selectively remove the secondary –OH group, while preserving the primary –OH groups in glycerol. Besides tungsten-based catalysts, Re-based catalysts developed by Tomishige's group demonstrate good performances in terms of hydrogenolysis activity and product selectivity.[146–148] Typically, over Ir–ReO_x/SiO_2 catalyst with H_2SO_4 being present, the 1,3-propanediol selectivity reaches *ca.* 60% at 30% glycerol conversion at 120 °C for 12 h at 8 MPa initial H_2 pressure. According to characterization and experimental results, the authors propose that glycerol is first adsorbed on the surface of a ReO_x cluster at the terminal position to 2,3-dihydroxypropoxide. Then, the heterolytic hydrogen atoms previously activated on Ir sites attack the secondary –OH of the 2,3-dihydroxypropoxide to form 3-hydroxypropoxide. Finally, the obtained 3-hydroxypropoxide is hydrolyzed to 1,3-propanediol (Fig. 17, left). The Re cluster shows a steric preference for the activation of the terminal –OH of glycerol, resulting in high 1,3-propanediol selectivity.[149] In a follow-up work, different strategies including the use of solid acidic H-ZSM-5 to replace the corrosive H_2SO_4 have been described. Metal loading was elevated to adjust the Re/metal ratio and the supports were changed to examine the interaction between the support and metal species. In this way, the yield of 1,3-propanediol was improved and the reaction mechanism for this reaction over Re-based catalysts was elucidated.[31,150] For instance, over the Ir–ReO_x/SiO_2 catalyst with a high Ir loading up to 20%, a high 1,3-propanediol selectivity of *ca.* 70% was obtained at 20% conversion of glycerol. Additionally, the high selectivity of 1,3-propanediol was almost independent of the glycerol concentrations. On the basis of XRD, EXAFS, and CO-FTIR analyses, the authors posit that the active site resides at the Ir–ReO_x interface, primarily situated at the periphery or vertex of Ir particles, as illustrated in Fig. 17 (right).

Besides the structure of Re species, the type of metal also greatly affects the product selectivity. For instance, 1,2-propanediol is preferably produced over Pt–ReO_x based catalysts. Under the reaction conditions, strong Brønsted acid sites are formed over the bimetallic catalyst, which catalyzes the dehydration of glycerol to aldehyde, followed by hydrogenation reactions over Pt sites.[151–153] Similarly, the addition of Pt on Ir–ReO_x/SiO_2 catalysts shifts the main product from 1,3-propanediol to 1,2-propanediol for glycerol conversions without hydrogen being present.[154] Over non-modified Ce-supported Re oxide catalysts (10 wt% ReO_x/CeO_2 + SiO_2), the deoxydehydration of glycerol to allyl alcohol is achieved with a yield up to 86%, using 2-hexanol and 4-methyl-2-pentanol as both a

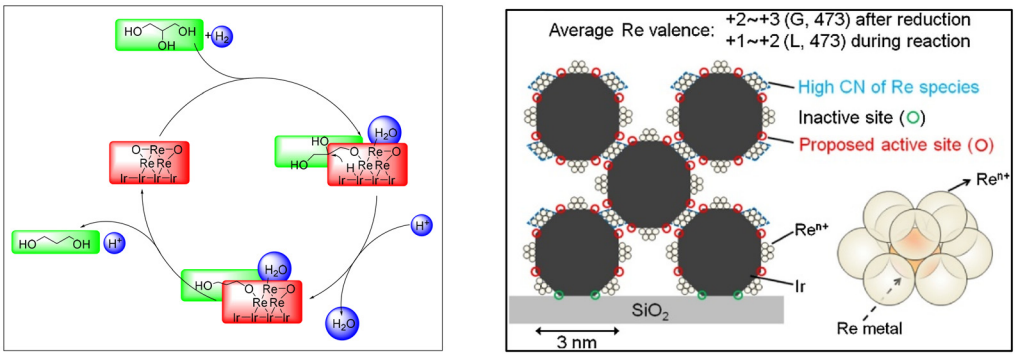

Fig. 17 Potential reaction pathway for glycerol hydrogenolysis over Ir–ReO_x/SiO_2 (left) and model structure of Ir–ReO_x/SiO_2 (20 wt%-Ir, Re/Ir = 0.34, actual) during the reaction (right).[149,150]

H-donor and a solvent at 175 °C. Based on the experimental results, the redox couples of Re^{VII}/Re^{V} and Re^{VI}/Re^{IV}, should be the active sites for this reaction.[155] Additionally, Re based catalysts have been applied in dehydration reactions. For instance, over Re_2O_7 catalysts, benzylic alcohols were dehydrated into styrenes in the presence of toluene, at 100 °C and under ambient atmosphere.[156] In a later work, the reactants were extended to a wide range of allylic, aliphatic, and homoallylic alcohols. Interestingly, the heterogeneous Re_2O_7 catalyst demonstrates superior activity and selectivity when compared to sulfuric acid and most common solid acids.[157]

Another attractive deoxygenation reaction is the catalytic deoxydehydration reaction, which removes vicinal hydroxyl groups and forms C=C double bonds with the help of a sacrificial reductant. Learning from the robust activity of homogeneous Re species in deoxydehydration reactions, Re-based heterogeneous catalysts were also synthesized for this reaction and showed excellent performances. In 2013, Denning *et al.* utilized ReO_x on carbon for the deoxydehydration of glycols into olefins, but these catalysts suffered from leaching issues.[158] Afterwards, more stable ReO_x nanoparticles and supported ReO_x were synthesized for deoxydehydration reactions. Under reaction conditions, a mixture of Re^{VII}, Re^{IV}, and Re^{0} species is formed in the presence of alcohols, providing a redox pool for deoxydehydration reactions with improved catalyst stability.[159–161]

To further improve the catalyst stability and activity, metals have been introduced into the ReO_x system. For instance, over ReO_x–Pd/CeO_2 catalysts, tetrahydrofuran is obtained with a selectivity >99% using 1,4-anhydroerythritol as the reactant, as reported by Tomishige's group. With the aid of metallic Pd sites, the high-valent Re species was reduced to Re^{IV} by H_2, which was coordinated with vicinal OH groups of 1,4-anhydroerythritol to diolate. After removing the –OH groups, the alkene can be hydrogenated to tetrahydrofuran over metallic Pd sites in the presence of hydrogen (Fig. 18).[21,162] In follow-up studies, additional metals including Au, Ag, Ni were introduced onto ReO_x/CeO_2 catalysts for the deoxydehydration of different vicinal diols, and also described achieving >90% yield of deoxydehydration products.[25,163–166]

Due to the versatile applications of 1,4-butanediol in the polyester sectors, the deoxydehydration reaction was applied in the conversion of erythritol or 1,4-anhydroerythritol to 1,4-butanediol. Over the physical mixture of ReO_x(Au)/CeO_2 + ReO_x/C, the 1,4-butanediol yield reaches 90% at 140 °C with H_2 as the reductant. Over ReO_x(Au)/CeO_2 as the catalyst, the rate-determining step of the deoxydehydration of 1,4-anhydroerythritol to 2,5-dihydrofuran has been described as being the activation of H_2 by ReO_x/C. Afterwards, the 2,5-dihydrofuran is isomerized to 2,3-dihydrofuran over ReO_x/C, which is then further hydrated to hydroxytetrahydrofuran and at last hydrogenated forming 1,4-butanediol.[167–169] Using more abundant erythritol as feedstock, the deoxydehydration reactions, dehydration and hydrogenation reactions were coupled, obtaining a selectivity of 33% to 1,4-butanediol with a conversion of 74.2% cover Ir–ReO_x/SiO_2 as the catalyst.[77] When changing the support to rutile-TiO_2, the yield of 1,4-butanediol slightly decreases but with a high selectivity, especially at low conversion levels.[170] According to kinetic analysis results, C–O bond cleavage shows lower activation energy than C–C bond cleavage, in the presence of ReO_x species, resulting in a high selectivity for erythritol to 1,4-butanediol conversion.[171,172] During the reaction kinetics study of deoxydehydration and hydrogenation of erythritol to butanediols and *n*-butane over the ReO_x–Pd/CeO_2 catalyst, Cao *et al.* proposed that the deactivation of catalyst should not be attributed to the deposition of organic species, but the aggregation of ReO_x species, as evidenced by Raman spectroscopy and supported by density functional theory calculations.[173]

Apart from these applications, Re-based catalysts have also been used in deoxydehydration of multiple –OH chemicals. For example, ReO_x/ZrO_2 catalysts effectively facilitate the deoxydehydration of D-glucaric acid into valuable adipic acid ester, achieving a high yield of up to 82% when combined with subsequent hydrogenation over Pd/C catalysts.[174] Additionally, a two-step pathway has been devised for converting glucose into adipic acid. In the first step, glucose is oxidized into glucaric acid over Pt/CNT catalysts, obtaining 82% product yield after 4 h at 60 °C and 1 MPa O_2 pressure. In the second step, the four –OH groups are removed from adipic acid *via* the deoxyde-

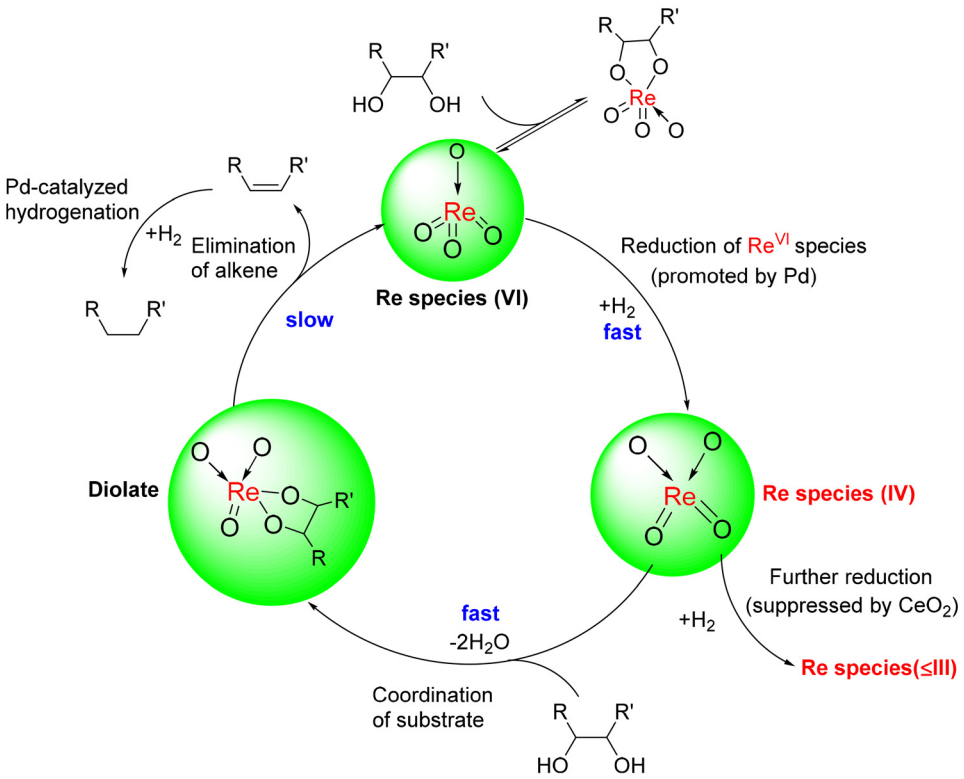

Fig. 18 Proposed reaction mechanism for the deoxydehydration reaction over ReO_x catalysts.[162]

hydration reaction over ReO_x/AC catalysts with yields up to 99%, and then the C=C bonds were hydrogenated to adipic acid over Pd sites. According to conditional experiments and density functional theory calculations, the authors propose a possible reaction mechanism for the second step (see Fig. 19). Initially, potassium glucarate dissolved in methanol undergoes esterification with methanol to form lactone and linear esters, facilitated by a solid acid catalyst. Subsequently, the ReO_x species, featuring the binuclear Re–O–Re site on ReO_3 surfaces, catalyzes the initial deoxydehydration reaction of methyl glucarate into corresponding olefins, concurrently oxidizing the Re–O–Re site. Following this, Pd nanoparticles facilitate the hydrogenation of the olefin by supplying active hydrogen through H_2 dissociation. Pd also facilitates the reduction of the oxidized rhenium sites with H_2. Finally, the saturated intermediates such as **1** and **2′** are transformed further into **2** with subsequent deoxydehydration and hydrogenation over ReO_x species and Pd nanoparticles to yield adipic acid.[175] With pure isopropanol as the solvent, a key hydrogen transfer agent, glucaric acid is efficiently converted into adipic acid over the same Pt–ReO_x/C catalyst *via* balancing the deoxydehydration and hydrogenation reactions.[176]

3.3.4 Direct hydrogenation of mixed bonds. Due to the versatile applications of ReO_x species in the activation of different bonds, they are used to upgrade biomass derived platform chemicals with multiple functional groups, typically for furfural and 5-hydroxymethylfurfural based chemical conversions. During the hydrogenolysis of furfural, 86.4% yield of 2-methylfuran is reached after 6 h at 200 °C over CuRe/γ-Al_2O_3 as the catalyst. The synergistic effect between Cu and Re active species is responsible for promoting the hydrogenolysis of the C–OH bond in furfuryl alcohol to produce 2-methylfuran, facilitated by a small amount of oxophilic Re species.[177] Due to the high activity of Ir–ReO_x/SiO_2 catalysts in hydrogenolysis of furfuryl alcohol, it is modified with Pd for the conversion of furfural to 1,5-pentanediol. Over the Pd–Ir–ReO_x/SiO_2 catalyst, the 1,5-pentanediol yield reaches 71.4% *via* a two-step reaction process. During the lower-temperature reaction step, furfural is hydrogenated to tetrahydrofurfuryl alcohol over ReO_x-modified Pd as catalyst. It is subsequently transformed into 1,5-pentanediol during the high-temperature step over ReO_x-modified Ir particles.[178,179] The Ir–ReO_x/SiO_2 catalyst is also described to be effective for the hydrodeoxygenation of furylmethanes to jet-fuel-range alkanes *via* hydrogenation of C=C, C–O and C=O bonds (Fig. 20). The Ir metal heterolytically dissociates H_2 for the hydrogenation of the furan rings, and then the strong synergy between Ir and ReO_x activates furan rings and alcoholic C–O bonds for hydrogenation to alkanes.[180]

5-Hydroxymethylfurfural can be hydrogenated to tetrahydropyran-2-methanol, which is further converted into 1,6-hexanediol at 84% yield over Rh–ReO_x/C as the catalyst. The ReO_x and Rh species show a synergistic effect between the Rh metal surface and attached ReO_x species for hydrogenolysis of tetrahydropyran-2-methanol to 1,6-hexanediol.[181] In another attempt, 5-hydroxymethylfurfural has been selectively converted into 1,6-hexanediol (1,6-hydrodeoxygenation) over the

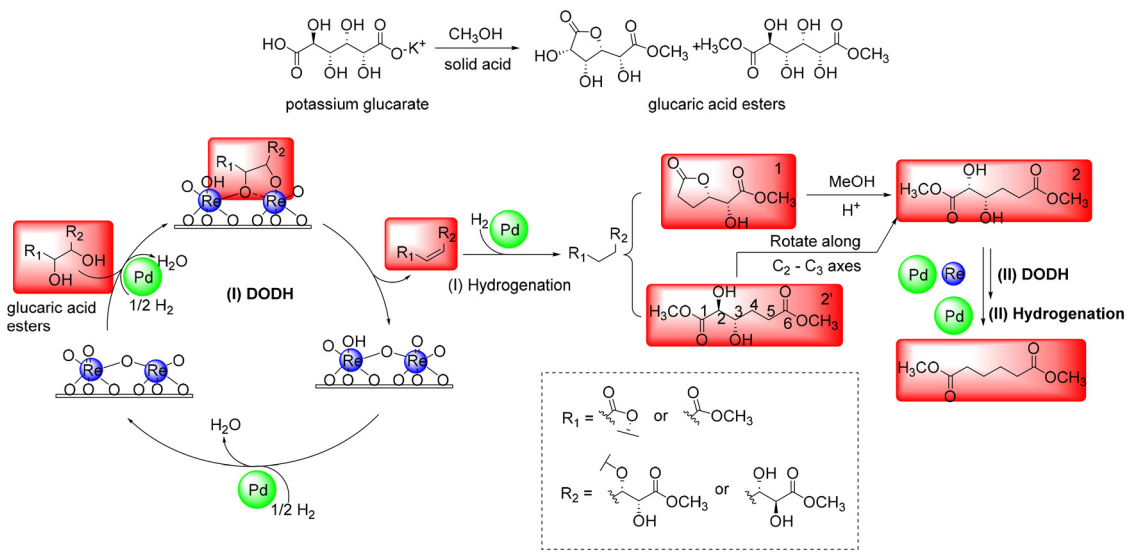

Fig. 19 Proposed reaction mechanism for the conversion of glucaric acid (potassium glucarate) to adipic acid (methyl adipate) catalyzed by Pd–ReO_x/AC[175] (DODH: deoxydehydration).

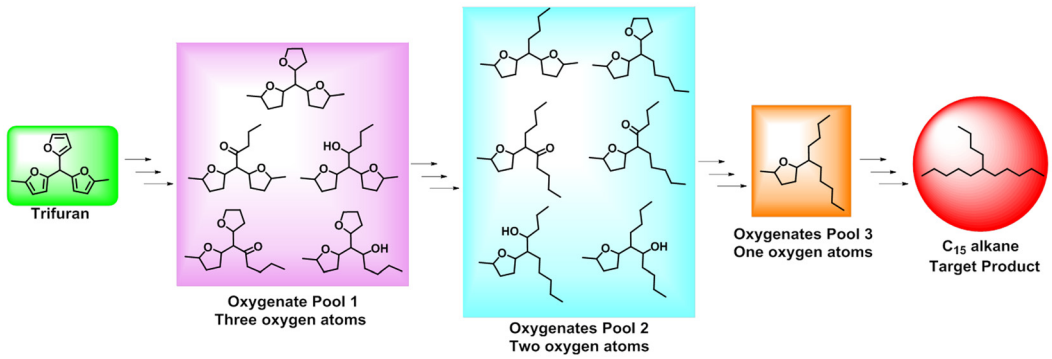

Fig. 20 Intermediate oxygen-containing compounds generated during the trifuran conversion process over an Ir–ReO_x/SiO_2 catalyst were discerned *via* GC-MS analysis of the resultant product solutions.[180]

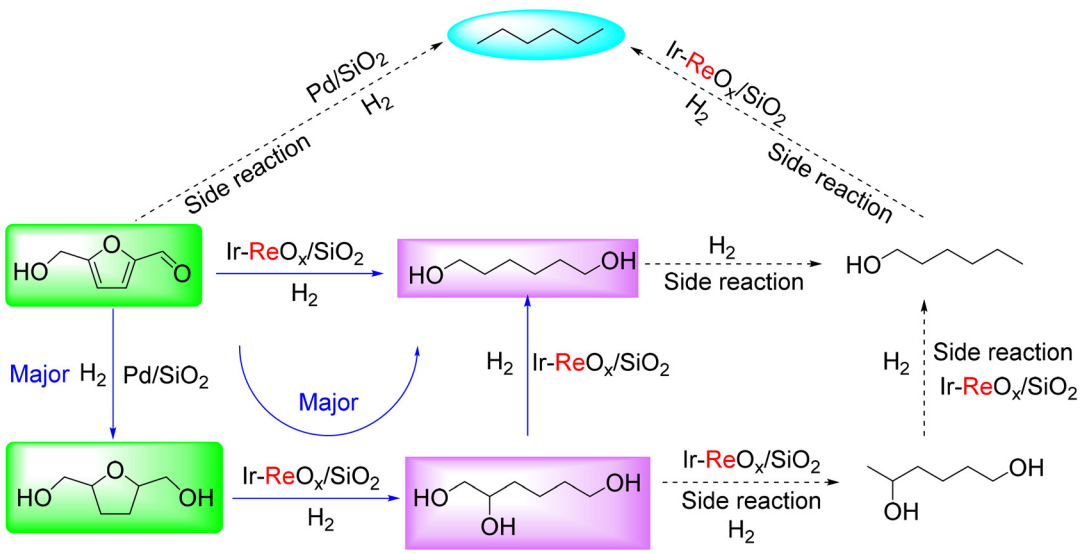

Fig. 21 Reaction routes of hydroxymethylfurfural conversion to 1,6-hydrodeoxygenation over Pd/SiO_2 + Ir–ReO_x/SiO_2 catalysts.[182]

double-layered catalysts of Pd/SiO_2 + $Ir–ReO_x/SiO_2$ in a fixed-bed reactor, obtaining yields as high of 57.8% at 100 °C and 7 MPa H_2. Remarkably, the double-layered catalysts exhibit superior performance when contrasted with single-layer catalysts such as $Pd–Ir–ReO_x/SiO_2$, despite containing an equivalent amount of active components. As shown in Fig. 21, the upper layer Pd/SiO_2 catalyzes the direct hydrogenation of 5-hydroxymethylfurfural to 2,5-bis(hydroxymethyl)-tetrahydrofuran, which are further hydrogenated into 1,6-hexandiol *via* the intermediate 1,2,6-hexanetriol over $Ir–ReO_x/SiO_2$ catalysts. Simultaneously, side reactions including the hydrodeoxygenation of products, reactants and intermediates take place, lowering the final product yield of 1,6-hexandiol.[182]

4. Conclusions and outlook

Re-based catalytic compounds have emerged as highly useful materials for various catalytic reactions, encompassing olefin metathesis, aldehyde olefination, oxidation, and dehydrogenation reactions. Biomass, recognized as a sustainable and renewable resource, serves as an ideal starting material for the production of value-added chemicals through catalytic processes. The integration of Re-based compounds with biomass conversion has been elegantly demonstrated in previous studies.

Due to rapid progress in this field, this work focuses on the catalysis of the three main components of lignocellulose (cellulose, hemicellulose, and lignin) and their derivatives through C–O bond cleavage, oxidation, hydrogenation, deoxydehydration, and hydrodeoxygenation reactions using Re-based compounds. The reaction pathways, catalytic systems, the key role of Re species in controlling product selectivity and the reaction mechanisms are listed and discussed. This provides insights into the delivery of value-added chemicals from biomass over Re catalysts. This review serves as a comprehensive approach for summarizing and capturing the key highlights, identifying knowledge gaps, and suggesting potential research directions for the advancing Re-catalyzed biomass conversion.

Although significant progress has been made, there are still some challenges in the application of Re-based catalysts in biomass conversions:

(1) Stability: different from other transition metals, Re-based catalysts demonstrate unique activity and selectivity in oxygen-containing feedstock conversions. However, leaching issues of Re-catalytic systems in both homogeneous and heterogeneous phases often occur. To date, keeping both high catalytic activity and stability still remains a huge challenge for Re-based catalysts. Thus, it is crucial to design supports with a uniform and well-defined surface structure so as to increase the interaction between Re sites. Thanks to the rapid development of novel porous materials such as metal organic frameworks (MOFs), covalent organic frameworks (COFs) and polymers, there are a number of options for highly dispersed Re catalysts synthesis with definite structures. Alternatively, synthesis of high stability Re single atom catalysts would be an appropriate strategy to maximize the Re activity per atom with every site featuring unique electronic structures, while preserving distinct metal support interactions. Here, single atom catalysis bridges the gap between homogeneous and heterogeneous catalysts and provides a unique viewpoint on Re catalysis.[183,184] For example, the Re–Ni–Fe alloy nanoparticles over lanthanum ferrite ($LaFeO_3$) showed long-term resistance to coking and sintering for methane dry reforming due to the inhibition of Re evaporation issues.[185] This alloy strategy provides valuable information for metallic Re catalysis and high-stability catalyst design.

(2) Mechanistic understanding: the incomplete understanding of catalytic behavior of Re-based catalysts hampers the discovery of real active sites for the catalytic reactions due to the polyvalent behavior of Re compounds. To elucidate the catalytic mechanisms, advancement of *in situ* and *operando* characterization techniques would be helpful for in-depth analysis. Biomass conversion reactions often take place in organic solvents, but their use poses challenges for *operando* characterization. The presence of liquid organic solvents can lead to interference due to their significant absorptions in infrared (IR) or ultraviolet-visible (UV/Vis) spectral ranges. Additionally, the high viscosity of organic solvents may have a strong impact on the mass transfer, reactant concentration and diffusion rates of the reactants. Therefore, the development of appropriate *operando* cells and techniques for the conversion in organic solvents remains an active area of research.

(3) New applications: the high electronic richness combined with the tunable stereochemical bulk of Re-based catalysts provides numerous opportunities in biomass reactions. The renewed interest in lignocellulose-based reactions catalyzed by Re-based compounds has led to the production of other value-added biochemicals. For instance, heteroatoms (X) participate in biomass conversion through the cleavage of C–O/C–C bonds and the construction of C–X bonds catalyzed by Re-based compounds, resulting in monomers containing heteroatoms. This expands the applications and functionalization of lignocellulosic production. Additionally, single Re atom catalysis is also an attractive option for biomass conversion due to its definite structure and active sites. The transformation of biomass-derived platform chemicals into high yields of a single monomer, rather than a mixture of products, should receive significant attention. Therefore, further advancements in designing Re-based catalysts for suitable reactions to access value-added monomers are crucial requirements for cost-competitive and sustainable large-scale production in industry.

(4) Economic feasibility: Re-catalyzed deoxydehydration has undergone significant advancements, particularly in the presence of a reductant, resulting in the production of olefin products. Assessments such as life cycle analysis, economic evaluation, and reaction efficiency are essential in determining the most suitable processes for industrial application. Given the high cost associated with Re metal, more efforts should be devoted on the following aspects: (1) developing inexpensive and abundantly available metals like molybdenum, vanadium, and tungsten holds promise for large-scale and economically viable deoxydehydration reactions. (2) Re based catalysts

should be efficient and recyclable to ensure sustainability and economic viability. (3) The Re sites should be 100% utilized, *i.e.* single Re catalysts for biomass conversions. These methodologies hold great potential for overcoming the current limitations and unlocking new opportunities for advancement in the field.

(5) Carbon neutrality: the recent achievements of Re-based catalysts for biomass conversion are beneficial for reaching the goal of carbon neutrality. First, the conversion of biomass to chemicals, fuels and materials reduces CO_2 emissions since biomass is the fixed CO_2 in the atmosphere *via* the photosynthesis process. Then, the Re-based catalysts demonstrate robust activity and efficiency in tailoring the –OH groups in biomass conversion. For instance, over Re-based catalysts, high olefin product yields were obtained through the deoxydehydration reaction, thus being a green and atom economic reaction for biomass conversion. Thereafter, the product separation energy and the treatment of waste water should be largely reduced. Finally, the rapid developments of Re catalysis also inspire the application of Re-based catalysts in other energy sectors, which will upgrade some energy systems and promote the construction of a low carbon-footprint society. For instance, atomically dispersed ReO_4 exhibited >93% selectivity to acetic acid for halide-free, gas phase carbonylation of methanol, representing a new class of promising catalysts for alcohol carbonylation.[186]

To tackle these persistent challenges, it is essential to foster close collaboration across various disciplines and facilitate dialogue between academia and industry. This review aims to spark significant interest among researchers in both Re chemistry and biomass conversion. It will encourage further exploration of Re-based compounds as promising alternative catalysts, thereby meeting the current and future needs of biomass conversion.

Data availability

No primary research results, software or code have been included and no new data were generated or analysed as part of this review.

Conflicts of interest

There are no conflicts to declare.

Acknowledgements

Support from the National Natural Science Foundation of China (22078317, 22378383) is acknowledged.

References

1 D. Welsby, J. Price, S. Pye and P. Ekins, *Nature*, 2021, **597**, 230–234.
2 M. S. Nazir, Z. M. Ali, M. Bilal, H. M. Sohail and H. M. N. Iqbal, *Environ. Sci. Pollut. Res.*, 2020, **27**, 33516–33526.
3 K. M. Yavor, V. Bach and M. Finkbeiner, *Sustainability*, 2021, **13**, 6107.
4 P. Gallezot, *Chem. Soc. Rev.*, 2012, **41**, 1538–1558.
5 Z. Zhang, J. Song and B. Han, *Chem. Rev.*, 2017, **117**, 6834–6880.
6 I. Delidovich, P. J. C. Hausoul, L. Deng, R. Pfützenreuter, M. Rose and R. Palkovits, *Chem. Rev.*, 2016, **116**, 1540–1599.
7 B. Zhang, B. K. Biswal, J. Zhang and R. Balasubramanian, *Chem. Rev.*, 2023, **123**, 7193–7294.
8 Y. Feng, S. Long, X. Tang, Y. Sun, R. Luque, X. Zeng and L. Lin, *Chem. Soc. Rev.*, 2021, **50**, 6042–6093.
9 C. Li, X. Zhao, A. Wang, G. W. Huber and T. Zhang, *Chem. Rev.*, 2015, **115**, 11559–11624.
10 Z. Sun, B. Fridrich, A. de Santi, S. Elangovan and K. Barta, *Chem. Rev.*, 2018, **118**, 614–678.
11 X. Wu, N. Luo, S. Xie, H. Zhang, Q. Zhang, F. Wang and Y. Wang, *Chem. Soc. Rev.*, 2020, **49**, 6198–6223.
12 G. Li, R. Wang, J. Pang, A. Wang, N. Li and T. Zhang, *Chem. Rev.*, 2024, **124**, 2889–2954.
13 R. Gérardy, D. P. Debecker, J. Estager, P. Luis and J.-C. M. Monbaliu, *Chem. Rev.*, 2020, **120**, 7219–7347.
14 A. A. Koutinas, A. Vlysidis, D. Pleissner, N. Kopsahelis, I. Lopez Garcia, I. K. Kookos, S. Papanikolaou, T. H. Kwan and C. S. K. Lin, *Chem. Soc. Rev.*, 2014, **43**, 2587–2627.
15 T. A. Ewing, N. Nouse, M. van Lint, J. van Haveren, J. Hugenholtz and D. S. van Es, *Green Chem.*, 2022, **24**, 6373–6405.
16 A. J. J. Straathof, *Chem. Rev.*, 2014, **114**, 1871–1908.
17 S. Dutta, *ChemSusChem*, 2012, **5**, 2125–2127.
18 J. Yi, S. Liu and M. M. Abu-Omar, *ChemSusChem*, 2012, **5**, 1401–1404.
19 J. R. Dilworth, *Coord. Chem. Rev.*, 2021, **436**, 213822.
20 G. K. Cook and M. A. Andrews, *J. Am. Chem. Soc.*, 1996, **118**, 9448–9449.
21 N. Ota, M. Tamura, Y. Nakagawa, K. Okumura and K. Tomishige, *Angew. Chem., Int. Ed.*, 2015, **54**, 1897–1900.
22 N. N. Tshibalonza and J.-C. M. Monbaliu, *Green Chem.*, 2020, **22**, 4801–4848.
23 L. J. Donnelly, S. P. Thomas and J. B. Love, *Chem. – Asian J.*, 2019, **14**, 3782–3790.
24 J. R. Dethlefsen and P. Fristrup, *ChemSusChem*, 2015, **8**, 767–775.
25 S. Tazawa, N. Ota, M. Tamura, Y. Nakagawa, K. Okumura and K. Tomishige, *ACS Catal.*, 2016, **6**, 6393–6397.
26 S. Raju, M.-E. Moret and R. J. M. Klein Gebbink, *ACS Catal.*, 2015, **5**, 281–300.
27 X. Huang, K. Liu, W. L. Vrijburg, X. Ouyang, A. Iulian Dugulan, Y. Liu, M. W. G. M. Tiny Verhoeven, N. A. Kosinov, E. A. Pidko and E. J. M. Hensen, *Appl. Catal., B*, 2020, **278**, 119314.
28 M. Tamura, K. Tokonami, Y. Nakagawa and K. Tomishige, *ACS Catal.*, 2016, **6**, 3600–3609.

29 M. L. Gothe, K. L. C. Silva, A. L. Figueredo, J. L. Fiorio, J. Rozendo, B. Manduca, V. Simizu, R. S. Freire, M. A. S. Garcia and P. Vidinha, *Eur. J. Inorg. Chem.*, 2021, 4043–4065.
30 Y. Nakagawa, K. Mori, K. Chen, Y. Amada, M. Tamura and K. Tomishige, *Appl. Catal., A*, 2013, **468**, 418–425.
31 Y. Nakagawa, X. Ning, Y. Amada and K. Tomishige, *Appl. Catal., A*, 2012, **433–434**, 128–134.
32 K. Chen, M. Tamura, Z. Yuan, Y. Nakagawa and K. Tomishige, *ChemSusChem*, 2013, **6**, 613–621.
33 S. Liu, Y. Okuyama, M. Tamura, Y. Nakagawa, A. Imai and K. Tomishige, *Green Chem.*, 2016, **18**, 165–175.
34 J. Cao, M. Tamura, Y. Nakagawa and K. Tomishige, *ACS Catal.*, 2019, **9**, 3725–3729.
35 K. A. DeNike and S. M. Kilyanek, *R. Soc. Open Sci.*, 2019, **6**, 191165.
36 K. Tomishige, M. Yabushita, J. Cao and Y. Nakagawa, *Green Chem.*, 2022, **24**, 5652–5690.
37 C. Boucher-Jacobs and K. M. Nicholas, in *Selective Catalysis for Renewable Feedstocks and Chemicals*, ed. K. M. Nicholas, 2014, vol. 353, pp. 163–184.
38 X. Li, B. Zhang, X. Pan, J. Ji, Y. Ren, H. Wang, N. Ji, Q. Liu and C. Li, *ChemSusChem*, 2020, **13**, 4409–4419.
39 B. Zhang, Z. Qi, X. Li, J. Ji, W. Luo, C. Li, A. Wang and T. Zhang, *ACS Sustainable Chem. Eng.*, 2019, **7**, 208–215.
40 X. Li, Y. Ding, X. Pan, Y. Xing, B. Zhang, X. Liu, Y. Tan, H. Wang and C. Li, *J. Energy Chem.*, 2022, **67**, 492–499.
41 B. Zhang, Z. Qi, X. Li, J. Ji, L. Zhang, H. Wang, X. Liu and C. Li, *Green Chem.*, 2019, **21**, 5556–5564.
42 Z. J. Qi, B. Zhang, J. W. Ji, X. X. Li, T. Dai, H. W. Guo, A. Q. Wang, L. C. Lu and C. Z. Li, *ChemPlusChem*, 2018, **83**, 500–505.
43 R. G. Harms, I. I. E. Markovits, M. Drees, W. A. Herrmann, M. Cokoja and F. E. Kühn, *ChemSusChem*, 2014, **7**, 429–434.
44 B. J. Hofmann, R. G. Harms, S. P. Schwaminger, R. M. Reich and F. E. Kuhn, *J. Catal.*, 2019, **373**, 190–200.
45 X. Li, Q. Qiang, Y. Ding, Y. Xing, J. Ji, H. Wang, X. Pan, B. Zhang and C. Li, *Chem. Eng. Sci.*, 2024, **285**, 119535.
46 F. Chen, X. Jiang, L. Zhang, R. Lang and B. Qiao, *Chin. J. Catal.*, 2018, **39**, 893–898.
47 J. R. Dilworth and S. J. Parrott, *Chem. Soc. Rev.*, 1998, **27**, 43–55.
48 K. K.-W. Lo, *Acc. Chem. Res.*, 2015, **48**, 2985–2995.
49 E. B. Bauer, A. A. Haase, R. M. Reich, D. C. Crans and F. E. Kühn, *Coord. Chem. Rev.*, 2019, **393**, 79–117.
50 W. A. Herrmann and F. E. Kühn, *Acc. Chem. Res.*, 1997, **30**, 169–180.
51 C. C. Romão, F. E. Kühn and W. A. Herrmann, *Chem. Rev.*, 1997, **97**, 3197–3246.
52 J. E. Fergusson, *Coord. Chem. Rev.*, 1966, **1**, 459–503.
53 S. Liu, A. Senocak, J. L. Smeltz, L. Yang, B. Wegenhart, J. Yi, H. I. Kenttämaa, E. A. Ison and M. M. Abu-Omar, *Organometallics*, 2013, **32**, 3210–3219.
54 T. J. Korstanje, J. T. B. H. Jastrzebski and R. J. M. Klein Gebbink, *Chem. – Eur. J.*, 2013, **19**, 13224–13234.
55 Y. Cai and J. H. Espenson, *Inorg. Chem.*, 2005, **44**, 489–495.
56 H. Kobayashi, T. Komanoya, S. K. Guha, K. Hara and A. Fukuoka, *Appl. Catal., A*, 2011, **409–410**, 13–20.
57 P. L. Dhepe and A. Fukuoka, *ChemSusChem*, 2008, **1**, 969–975.
58 R. Rinaldi and F. Schüth, *ChemSusChem*, 2009, **2**, 1096–1107.
59 M. Shiramizu and F. D. Toste, *Angew. Chem., Int. Ed.*, 2012, **51**, 8082–8086.
60 J. Li, M. Lutz and R. J. M. Klein Gebbink, *Catal. Sci. Technol.*, 2020, **10**, 3782–3788.
61 J. Li, M. Lutz, M. Otte and R. J. M. Klein Gebbink, *ChemCatChem*, 2018, **10**, 4755–4760.
62 E. S. Koh, T. H. Lee, D. Y. Lee, H. J. Kim, Y. W. Ryu and J. H. Seo, *Biotechnol. Lett.*, 2003, **25**, 2103–2105.
63 I. Ahmad, G. Chapman and K. M. Nicholas, *Organometallics*, 2011, **30**, 2810–2818.
64 C. Boucher-Jacobs and K. M. Nicholas, *Organometallics*, 2015, **34**, 1985–1990.
65 L. G. Possato, T. F. Chaves, W. H. Cassinelli, S. H. Pulcinelli, C. V. Santilli and L. Martins, *Catal. Today*, 2017, **289**, 20–28.
66 J. Mazarío, P. Concepción, M. Ventura and M. E. Domine, *J. Catal.*, 2020, **385**, 160–175.
67 M. El Doukkali, A. Iriondo and I. Gandarias, *Mol. Catal.*, 2020, **490**, 110928.
68 G. Scioli, L. Tonucci, P. Di Profio, A. Proto, R. Cucciniello and N. d'Alessandro, *Sustainable Chem. Pharm.*, 2020, **17**, 100273.
69 D. Taher, M. E. Thibault, D. Di Mondo, M. Jennings and M. Schlaf, *Chem. – Eur. J.*, 2009, **15**, 10132–10143.
70 V. Canale, L. Tonucci, M. Bressan and N. d'Alessandro, *Catal. Sci. Technol.*, 2014, **4**, 3697–3704.
71 C. Boucher-Jacobs and K. M. Nicholas, *ChemSusChem*, 2013, **6**, 597–599.
72 M. Lupacchini, A. Mascitti, V. Canale, L. Tonucci, E. Colacino, M. Passacantando, A. Marrone and N. d'Alessandro, *Catal. Sci. Technol.*, 2019, **9**, 3036–3046.
73 X. Li, D. Wu, T. Lu, G. Yi, H. Su and Y. Zhang, *Angew. Chem., Int. Ed.*, 2014, **53**, 4200–4204.
74 M. Shiramizu and F. D. Toste, *Angew. Chem., Int. Ed.*, 2013, **52**, 12905–12909.
75 X. Li and Y. Zhang, *ChemSusChem*, 2016, **9**, 2774–2778.
76 E. Arceo, J. A. Ellman and R. G. Bergman, *J. Am. Chem. Soc.*, 2010, **132**, 11408–11409.
77 Y. Amada, H. Watanabe, Y. Hirai, Y. Kajikawa, Y. Nakagawa and K. Tomishige, *ChemSusChem*, 2012, **5**, 1991–1999.
78 S. Qu, Y. Dang, M. Wen and Z.-X. Wang, *Chem. – Eur. J.*, 2013, **19**, 3827–3832.
79 L. Lai, M. Liu, J. Liu, W. Li, W. Miao, Z. Sun, Z. Wang, Y. Wang, H. Shi, C. Chen, X. Jin and C. Yang, *ACS Sustainable Chem. Eng.*, 2023, **11**, 15851–15864.
80 S. Gillet, M. Aguedo, L. Petitjean, A. R. C. Morais, A. M. da Costa Lopes, R. M. Lukasik and P. T. Anastas, *Green Chem.*, 2017, **19**, 4200–4233.

81 J. Zakzeski, P. C. A. Bruijnincx, A. L. Jongerius and B. M. Weckhuysen, *Chem. Rev.*, 2010, **110**, 3552–3599.
82 R. Rinaldi, R. Jastrzebski, M. T. Clough, J. Ralph, M. Kennema, P. C. A. Bruijnincx and B. M. Weckhuysen, *Angew. Chem., Int. Ed.*, 2016, **55**, 8164–8215.
83 S. S. Wong, R. Shu, J. Zhang, H. Liu and N. Yan, *Chem. Soc. Rev.*, 2020, **49**, 5510–5560.
84 C. Xu, R. A. D. Arancon, J. Labidi and R. Luque, *Chem. Soc. Rev.*, 2014, **43**, 7485–7500.
85 M. M. Abu-Omar, K. Barta, G. T. Beckham, J. S. Luterbacher, J. Ralph, R. Rinaldi, Y. Román-Leshkov, J. S. M. Samec, B. F. Sels and F. Wang, *Energy Environ. Sci.*, 2021, **14**, 262–292.
86 C. Crestini, P. Pro, V. Neri and R. Saladino, *Bioorg. Med. Chem.*, 2005, **13**, 2569–2578.
87 C. Crestini, M. C. Caponi, D. S. Argyropoulos and R. Saladino, *Bioorg. Med. Chem.*, 2006, **14**, 5292–5302.
88 B. Zhang, C. Li, T. Dai, G. W. Huber, A. Wang and T. Zhang, *RSC Adv.*, 2015, **5**, 84967–84973.
89 J. M. Nichols, L. M. Bishop, R. G. Bergman and J. A. Ellman, *J. Am. Chem. Soc.*, 2010, **132**, 12554–12555.
90 A. Fukuoka and P. L. Dhepe, *Angew. Chem., Int. Ed.*, 2006, **45**, 5161–5163.
91 C. Luo, S. Wang and H. Liu, *Angew. Chem., Int. Ed.*, 2007, **46**, 7636–7639.
92 N. Ji, T. Zhang, M. Zheng, A. Wang, H. Wang, X. Wang and J. G. Chen, *Angew. Chem., Int. Ed.*, 2008, **47**, 8510–8513.
93 S. Liu, M. Tamura, Y. Nakagawa and K. Tomishige, *ACS Sustainable Chem. Eng.*, 2014, **2**, 1819–1827.
94 S. Liu, Y. Okuyama, M. Tamura, Y. Nakagawa, A. Imai and K. Tomishige, *ChemSusChem*, 2015, **8**, 628–635.
95 M. Tamura, N. Yuasa, J. Cao, Y. Nakagawa and K. Tomishige, *Angew. Chem., Int. Ed.*, 2018, **57**, 8058–8062.
96 J. R. Bernardo, M. C. Oliveira and A. C. Fernandes, *Mol. Catal.*, 2019, **465**, 87–94.
97 M. Chia, B. J. O'Neill, R. Alamillo, P. J. Dietrich, F. H. Ribeiro, J. T. Miller and J. A. Dumesic, *J. Catal.*, 2013, **308**, 226–236.
98 S. Avramescu, C. D. Ene, M. Ciobanu, J. Schnee, F. Devred, C. Bucur, E. Vasile, L. Colaciello, R. Richards, E. M. Gaigneaux and M. N. Verziu, *Catal. Sci. Technol.*, 2022, **12**, 167–180.
99 E. Blanco, A. B. Dongil, J. L. García-Fierro and N. Escalona, *Appl. Catal., A*, 2020, **599**, 117600.
100 P. Sirous-Rezaei, J. Jae, J.-M. Ha, C. H. Ko, J. M. Kim, J.-K. Jeon and Y.-K. Park, *Green Chem.*, 2018, **20**, 1472–1483.
101 I. T. Ghampson, G. Pecchi, J. L. G. Fierro, A. Videla and N. Escalona, *Appl. Catal., B*, 2017, **208**, 60–74.
102 F. Yang, D. Liu, H. Wang, X. Liu, J. Han, Q. Ge and X. Zhu, *J. Catal.*, 2017, **349**, 84–97.
103 X. Wang, W. Zhou, Y. Wang, S. Huang, Y. Zhao, S. Wang and X. Ma, *Catal. Today*, 2021, **365**, 223–234.
104 C. W. Park, J. W. Kim, H. U. Kim, Y.-K. Park, S. S. Lam, J.-M. Ha and J. Jae, *Int. J. Energy Res.*, 2021, **45**, 16349–16361.
105 L. Dong, L. Lin, X. Han, X. Si, X. Liu, Y. Guo, F. Lu, S. Rudić, S. F. Parker, S. Yang and Y. Wang, *Chem*, 2019, **5**, 1521–1536.
106 S. Totong, W. Laosiripojana, N. Laosiripojana and P. Daorattanachai, *Ind. Eng. Chem. Res.*, 2022, **61**, 215–223.
107 J. Hu, S. Zhang, R. Xiao, X. Jiang, Y. Wang, Y. Sun and P. Lu, *Bioresour. Technol.*, 2019, **279**, 228–233.
108 P. Sirous-Rezaei, D. Creaser and L. Olsson, *Appl. Catal., B*, 2021, **297**, 120449.
109 M. Tudorache, C. Opris, B. Cojocaru, N. G. Apostol, A. Tirsoaga, S. M. Coman, V. I. Parvulescu, B. Duraki, F. Krumeich and J. A. van Bokhoven, *ACS Sustainable Chem. Eng.*, 2018, **6**, 9606–9618.
110 C. Opris, B. Cojocaru, N. Gheorghe, M. Tudorache, S. M. Coman, V. I. Parvulescu, B. Duraki, F. Krumeich and J. A. van Bokhoven, *ACS Catal.*, 2017, **7**, 3257–3267.
111 G. Guo, W. Li, X. Dou, A. T. Ogunbiyi, T. Ahmed, B. Zhang and M. Wu, *Bioresour. Technol.*, 2021, **321**, 124443.
112 C. Herrera, I. T. Ghampson, K. Cruces, C. Sepúlveda, L. Barrientos, D. Laurenti, C. Geantet, R. Serpell, D. Contreras, V. Melin and N. Escalona, *Fuel*, 2020, **259**, 116245.
113 L. Kong, L. Zhang, J. Gu, L. Gou, L. Xie, Y. Wang and L. Dai, *Bioresour. Technol.*, 2020, **299**, 122582.
114 X. She, H. M. Brown, X. Zhang, B. K. Ahring and Y. Wang, *ChemSusChem*, 2011, **4**, 1071–1073.
115 M. Rimoldi, J. T. Hupp and O. K. Farha, *ACS Appl. Mater. Interfaces*, 2017, **9**, 35067–35074.
116 J. Pritchard, G. A. Filonenko, R. van Putten, E. J. M. Hensen and E. A. Pidko, *Chem. Soc. Rev.*, 2015, **44**, 3808–3833.
117 T. J. Korstanje, J. I. van der Vlugt, C. J. Elsevier and B. de Bruin, *Science*, 2015, **350**, 298–302.
118 H. S. Broadbent, G. C. Campbell, W. J. Bartley and J. H. Johnson, *J. Org. Chem.*, 1959, **24**, 1847–1854.
119 B. Rozmysłowicz, A. Kirilin, A. Aho, H. Manyar, C. Hardacre, J. Wärnå, T. Salmi and D. Y. Murzin, *J. Catal.*, 2015, **328**, 197–207.
120 Y. Takeda, Y. Nakagawa and K. Tomishige, *Catal. Sci. Technol.*, 2012, **2**, 2221–2223.
121 Y. Takeda, M. Tamura, Y. Nakagawa, K. Okumura and K. Tomishige, *ACS Catal.*, 2015, **5**, 7034–7047.
122 S. Liu, T. Simonetti, W. Zheng and B. Saha, *ChemSusChem*, 2018, **11**, 1446–1454.
123 K. Ralphs, G. Collins, H. Manyar, S. L. James and C. Hardacre, *ACS Sustainable Chem. Eng.*, 2022, **10**, 6934–6941.
124 X. Cao, J. Zhao, F. Long, P. Liu, X. Jiang, X. Zhang, J. Xu and J. Jiang, *Appl. Catal., B*, 2022, **312**, 121437.
125 L. Zhou, W. Lin, K. Liu, Z. Wang, Q. Liu, H. Cheng, C. Zhang, M. Arai and F. Zhao, *Catal. Sci. Technol.*, 2020, **10**, 222–230.
126 A. Corma, S. Iborra and A. Velty, *Chem. Rev.*, 2007, **107**, 2411–2502.
127 X. Di, Z. Shao, C. Li, W. Li and C. Liang, *Catal. Sci. Technol.*, 2015, **5**, 2441–2448.
128 U. G. Hong, H. W. Park, J. Lee, S. Hwang, J. Yi and I. K. Song, *Appl. Catal., A*, 2012, **415–416**, 141–148.

129 B. K. Ly, D. P. Minh, C. Pinel, M. Besson, B. Tapin, F. Epron and C. Especel, *Top. Catal.*, 2012, **55**, 466–473.
130 K. H. Kang, U. G. Hong, Y. Bang, J. H. Choi, J. K. Kim, J. K. Lee, S. J. Han and I. K. Song, *Appl. Catal., A*, 2015, **490**, 153–162.
131 Y. Takeda, M. Tamura, Y. Nakagawa, K. Okumura and K. Tomishige, *Catal. Sci. Technol.*, 2016, **6**, 5668–5683.
132 X. Di, C. Li, G. Lafaye, C. Especel, F. Epron and C. Liang, *Catal. Sci. Technol.*, 2017, **7**, 5212–5223.
133 B. K. Ly, B. Tapin, M. Aouine, P. Delichere, F. Epron, C. Pinel, C. Especel and M. Besson, *ChemCatChem*, 2015, **7**, 2161–2178.
134 J. M. Keels, X. Chen, S. Karakalos, C. Liang, J. R. Monnier and J. R. Regalbuto, *ACS Catal.*, 2018, **8**, 6486–6494.
135 B. Tapin, B. Khanh Ly, C. Canaff, F. Epron, C. Pinel, M. Besson and C. Especel, *Mater. Chem. Phys.*, 2020, **252**, 123225.
136 M. Sajid, U. Farooq, G. Bary, M. M. Azim and X. Zhao, *Green Chem.*, 2021, **23**, 9198–9238.
137 W.-P. Xu, X.-F. Chen, H.-J. Guo, H.-L. Li, H.-R. Zhang, L. Xiong and X.-D. Chen, *J. Chem. Technol. Biotechnol.*, 2021, **96**, 3009–3024.
138 R. Bassi, P. Baeza, C. Sepulveda, I. T. Ghampson, E. Camu, A. Brückner, U. Bentrup, J. L. G. Fierro and N. Escalona, *Appl. Catal., A*, 2021, **625**, 118328.
139 D. Lee, H. U. Kim, J. R. Kim, Y.-K. Park, J.-M. Ha and J. Jae, *J. Ind. Eng. Chem.*, 2024, **131**, 490–502.
140 R. Bacchiocchi, J. De Maron, T. Tabanelli, D. Bianchi and F. Cavani, *Sustainable Energy*, 2023, **7**, 671–681.
141 L. Luo, Y. Ma, Y. He, J. Wang, T. Xue, H. Wu, Y. Guan and P. Wu, *Fuel*, 2023, **344**, 128028.
142 S. T. Thompson and H. H. Lamb, *ACS Catal.*, 2016, **6**, 7438–7447.
143 F. Toledo, I. T. Ghampson, C. Sepúlveda, R. García, J. L. G. Fierro, A. Videla, R. Serpell and N. Escalona, *Fuel*, 2019, **242**, 532–544.
144 K. Tomishige, Y. Nakagawa and M. Tamura, *Chin. Chem. Lett.*, 2020, **31**, 1071–1077.
145 Y. Liu, B. Zhong and A. Lawal, *RSC Adv.*, 2022, **12**, 27997–28008.
146 Y. Shinmi, S. Koso, T. Kubota, Y. Nakagawa and K. Tomishige, *Appl. Catal., B*, 2010, **94**, 318–326.
147 Y. Amada, Y. Shinmi, S. Koso, T. Kubota, Y. Nakagawa and K. Tomishige, *Appl. Catal., B*, 2011, **105**, 117–127.
148 Y. Amada, H. Watanabe, M. Tamura, Y. Nakagawa, K. Okumura and K. Tomishige, *J. Phys. Chem.*, 2012, **116**, 23503–23514.
149 Y. Nakagawa, Y. Shinmi, S. Koso and K. Tomishige, *J. Catal.*, 2010, **272**, 191–194.
150 L. Liu, T. Asano, Y. Nakagawa, M. Tamura, K. Okumura and K. Tomishige, *ACS Catal.*, 2019, **9**, 10913–10930.
151 C. Deng, X. Duan, J. Zhou, D. Chen, X. Zhou and W. Yuan, *Catal. Today*, 2014, **234**, 208–214.
152 D. D. Falcone, J. H. Hack, A. Y. Klyushin, A. Knop-Gericke, R. Schlögl and R. J. Davis, *ACS Catal.*, 2015, **5**, 5679–5695.
153 V. Korpelin, G. Sahoo, R. Ikonen and K. Honkala, *J. Catal.*, 2023, **422**, 12–23.
154 S. Liu, M. Tamura, Z. Shen, Y. Zhang, Y. Nakagawa and K. Tomishige, *Catal. Today*, 2018, **303**, 106–116.
155 K. S. Vargas, J. Zaffran, M. Araque, M. Sadakane and B. Katryniok, *Mol. Catal.*, 2023, **535**, 112856.
156 T. J. Korstanje, J. T. B. H. Jastrzebski and R. J. M. Klein Gebbink, *ChemSusChem*, 2010, **3**, 695–697.
157 T. J. Korstanje, E. F. de Waard, J. T. B. H. Jastrzebski and R. J. M. Klein Gebbink, *ACS Catal.*, 2012, **2**, 2173–2181.
158 A. L. Denning, H. Dang, Z. Liu, K. M. Nicholas and F. C. Jentoft, *ChemCatChem*, 2013, **5**, 3567–3570.
159 L. Sandbrink, E. Klindtworth, H.-U. Islam, A. M. Beale and R. Palkovits, *ACS Catal.*, 2016, **6**, 677–680.
160 J. H. Jang, H. Sohn, J. Camacho-Bunquin, D. Yang, C. Y. Park, M. Delferro and M. M. Abu-Omar, *ACS Sustainable Chem. Eng.*, 2019, **7**, 11438–11447.
161 I. Meiners, Y. Louven and R. Palkovits, *ChemCatChem*, 2021, **13**, 2393–2397.
162 N. Ota, M. Tamura, Y. Nakagawa, K. Okumura and K. Tomishige, *ACS Catal.*, 2016, **6**, 3213–3226.
163 J. Cao, M. Tamura, R. Hosaka, A. Nakayama, J.-y. Hasegawa, Y. Nakagawa and K. Tomishige, *ACS Catal.*, 2020, **10**, 12040–12051.
164 K. Yamaguchi, Y. Nakagawa, C. Li, M. Yabushita and K. Tomishige, *ACS Catal.*, 2022, **12**, 12582–12595.
165 K. Yamaguchi, J. Cao, M. Betchaku, Y. Nakagawa, M. Tamura, A. Nakayama, M. Yabushita and K. Tomishige, *ChemSusChem*, 2022, **15**, e202102663.
166 Y. Nakagawa, S. Tazawa, T. Wang, M. Tamura, N. Hiyoshi, K. Okumura and K. Tomishige, *ACS Catal.*, 2017, **8**, 584–595.
167 T. Wang, S. Liu, M. Tamura, Y. Nakagawa, N. Hiyoshi and K. Tomishige, *Green Chem.*, 2018, **20**, 2547–2557.
168 T. Wang, M. Tamura, Y. Nakagawa and K. Tomishige, *ChemSusChem*, 2019, **12**, 3615–3626.
169 T. Wang, Y. Nakagawa, M. Tamura, K. Okumura and K. Tomishige, *React. Chem. Eng.*, 2020, **5**, 1237–1250.
170 M. Gu, L. Liu, Y. Nakagawa, C. Li, M. Tamura, Z. Shen, X. Zhou, Y. Zhang and K. Tomishige, *ChemSusChem*, 2021, **14**, 642–654.
171 E. M. Virgilio, M. E. Sad and C. L. Padró, *Appl. Catal., A*, 2022, **643**, 118691.
172 E. M. Virgilio, C. L. Padró and M. E. Sad, *ChemCatChem*, 2023, **15**, e202201618.
173 J. Cao, S. Larasati, M. Yabushita, Y. Nakagawa, J. Wärnå, D. Y. Murzin, D. Asada, A. Nakayama and K. Tomishige, *ACS Catal.*, 2024, **14**, 1663–1677.
174 J. Lin, H. Song, X. Shen, B. Wang, S. Xie, W. Deng, D. Wu, Q. Zhang and Y. Wang, *Chem. Commun.*, 2019, **55**, 11017–11020.
175 W. Deng, L. Yan, B. Wang, Q. Zhang, H. Song, S. Wang, Q. Zhang and Y. Wang, *Angew. Chem., Int. Ed.*, 2021, **60**, 4712–4719.
176 J. H. Jang, I. Ro, P. Christopher and M. M. Abu-Omar, *ACS Catal.*, 2021, **11**, 95–109.

177 J. Chuseang, R. Nakwachara, M. Kalong, S. Ratchahat, W. Koo-amornpattana, W. Klysubun, P. Khemthong, K. Faungnawakij, S. Assabumrungrat, V. Itthibenchapong and A. Srifa, *Sustainable Energy*, 2021, **5**, 1379–1393.
178 S. Liu, Y. Amada, M. Tamura, Y. Nakagawa and K. Tomishige, *Green Chem.*, 2014, **16**, 617–626.
179 K. Chen, K. Mori, H. Watanabe, Y. Nakagawa and K. Tomishige, *J. Catal.*, 2012, **294**, 171–183.
180 S. Liu, S. Dutta, W. Zheng, N. S. Gould, Z. Cheng, B. Xu, B. Saha and D. G. Vlachos, *ChemSusChem*, 2017, **10**, 3225–3234.
181 K. Chen, S. Koso, T. Kubota, Y. Nakagawa and K. Tomishige, *ChemCatChem*, 2010, **2**, 547–555.
182 B. Xiao, M. Zheng, X. Li, J. Pang, R. Sun, H. Wang, X. Pang, A. Wang, X. Wang and T. Zhang, *Green Chem.*, 2016, **18**, 2175–2184.
183 X. Zhang, L. Shang, Z. Yang and T. Zhang, *ChemPlusChem*, 2021, **86**, 1635–1639.
184 X.-Z. Yue, Y.-C. Liu, B.-A. Lu, X. Du, W. Lei, Z.-Y. Liu, S.-S. Yi and C. Lu, *Energy Environ. Sci.*, 2024, **17**, 5892–5900.
185 D. Zubenko, S. Singh and B. A. Rosen, *Appl. Catal., B*, 2017, **209**, 711–719.
186 J. Qi, J. Finzel, H. Robatjazi, M. Xu, A. S. Hoffman, S. R. Bare, X. Pan and P. Christopher, *J. Am. Chem. Soc.*, 2020, **142**, 14178–14189.